TECHNICAL UNIVERSITY OF CRETE
SCHOOL OF PRODUCTION
ENGINEERING AND
MANAGEMENT

MASTER THESIS

Integrated Traffic Control for Motorways using Variable Speed Limits and Lane Change Control Actions

Author

Vasileios MARKANTONAKIS

Supervisor

Prof. Ioannis PAPAMICHAIL

Thesis submitted in partial fullfillment of the requirements for the

degree of Master of Science

Chania, 2018

Contents

List of Figures

List of Tables

Acknowledgements

The completion of this thesis would not have been possible without the time, support and dedication of the people involved from the beginning of my postgraduate life. To start, I would like to express my sincere gratitude to my supervisor Professor Ioannis Papamichail for the continuous support, patience and guidance. Moreover, I want to express my gratitude to Professor Markos Papageorgiou for sharing his immense knowledge in the field of transportation. Finally, I want to thank my parents, my sister and my brother for encouraging me and inspiring me to follow my dreams.

Abstract

The wide deployment of Vehicle Automation and Communication Systems (VACS) in the following decade is expected to affect traffic performance on freeways. Apart from safety and comfort, one of the goals is the alleviation of traffic congestion that is a major and challenging problem for modern societies. This paper investigates the use of two feedback control strategies utilizing VACS in different penetration rates as well as their integrated use, aiming at maximising throughput at bottleneck locations. The first control strategy employs mainstream traffic flow control using appropriate variable speed limits as an actuator. The second control strategy delivers appropriate lane-changing actions to selected connected vehicles using a feedback-feedforward control law. Investigations of the proposed schemes have been conducted using a microscopic simulation model for a hypothetical freeway featuring a lane-drop bottleneck. The produced results demonstrate significant improvements even for low penetration rates.

CHAPTER 1

Introduction

Motorway traffic congestion, typically initiated at bottleneck locations, is a major problem for modern societies, causing serious infrastructure degradation [1]. Longer travel times, lower speeds, long queues in the network, are also a few of the immediate consequences. The most efficient way to mitigate this problem, since the existing motorways are underutilised especially in periods of high demand due to congestion, is the development and implementation of proper traffic control strategies [2].

Bottleneck locations can be freeway merge areas, areas with a particular infrastructure layout (such as lane drops, strong grade or curvature, tunnels or bridges etc.), areas with specific traffic conditions (e.g. strong weaving of traffic streams) or areas with external capacity-reducing events (e.g. work-zones, incidents). If the arriving demand is higher than the bottlneck capacity, the bottleneck is activated, i.e. congestion is formed upstream of the bottleneck location. It should be emphasised, however, that, according to empirical investigations [3], capacity flow in conventional traffic is not

reached simultaneously at all lanes. Thus, traffic breakdown may occur on one lane, while capacity reserves are still available on other lanes. This implies that the potentially achievable cross-lane capacity is not fully exploited. Naturally, once congestion appears on one lane, it spreads fast to the other lanes as well, as drivers on the affected lane attempt to escape the speed drop via lane changing. After congestion has occured, retarded and different vehicle acceleration at the congestion head causes the so-called capacity drop phenomenon, which breeds a reduction in the mainstream flow of a motorway, while a queue is forming upstream of the bottleneck location.

In the near future, Vehicle Automation and Communication Systems (VACS) are expected to revolutionise the features and capabilities of individual vehicles. The new features can be exploited via recommending, supporting, or even executing appropriately designed traffic control tasks [4]. Vehicles equipped with VACS may act both as sensors (providing information on traffic conditions) and as actuators, permitting the deployment of strategies like variable speed limits (VSL) and lane-changing control (LCC). Note that, while VSL control is feasible by means of conventional control infrastructure, employing Variable Message Signs (VMS), LCC is not feasible with conventional means, because it calls for the possibility to communicate with few individual vehicles, rather than with the whole vehicle polulationas by use of VMS. This thesis proposes and invesigates via microscopic simulation on a hypothetical motorway stretch the integrated use of two feedback control strategies utilizing VACS in different penetration rates, aiming at maximising throughput at bottleneck locations. The first control strategy employs Mainstream Traffic Flow Control (MTFC) using appropriate VSL that are

communicated to all connected vehicles. The second control strategy delivers appropriate lane-changing actions to selected connected vehicles.

CHAPTER 2

Microscopic Simulator

Over the last decades reasearchers and transport planners, are using mathematical modelling for resresenting transportation systems. Microscopic simulations is the most efficient way to assess and solve many transportation problems because simulation is safer, less expensive and faster than field implementation and testing [5]. Initially, simulation models must be carefully calibrated and validated, to provide reliable results. Calibrating a microscopic model is a time consuming process that requires accuracy to the parameters. Additionally validation provides assurance that the model reacts correctly within the acceptable criteria.

2.1 Introduction

Our investigations based on the proposed strategies were conducted using the AIMSUN Microscopic Simulator. AIMSUN (Advanced Interactive Microscopic Simulator for Urban and Non-urban Networks) [6] is a commercial high detail traffic forecasting

solution software, widely used due to it's high customization capabilities. A part of it's modelling features including traffic network development, different types of vehicles and drivers, speed detectors, are provided using a graphical user interface, that allows the user to model anything from a single intersection to an entire region, using all the equipment present in real traffic networks.

2.2 Behavioral Models

Microscopic simulation models consider individual driver and vehicle units in the traffic stream. During a simulation run, vehicles are moved through the network on the paths between the vehicles' origin and destination. Interactions between individual vehicles and between vehicles and the infrastructure are modelled during this process through equations designed to mimic real driver behaviour. These equations are commonly organised into sub-models that handle specific parts of the driving task. Car-following and lane-changing models are examples of sub-models [7]. A car following model is capable of controlling a vehicle's trajectory in the simulated road network, interacting with other vehicles at the same lane and lane changing orders or recommendations are received from a lane changing model to all simulated vehicles in the road network.

2.3 Car-Following Model

During a simulation run, each vehicle that enters the network updates it's acceleration and deceleration every simulation step using a car following model, that is selected at

the beginning of the simulation. Each driver responds to the surrounding traffic by means of an acceleration strategy towards a desired velocity in the free-flow regime, a braking strategy for approaching other vehicles or obstacles, and a car-driving strategy for maintaining a safe distance when driving behind another vehicle [8]. Microscopic traffic models typically assume that human drivers react to the stimulus from neighboring vehicles with the dominant influence originating from the directly leading vehicle known as "follow-the-leader" or "car-following" approximation [8]. The car-following strategy of the Aimsun simulator is based on the Gipps Car-Following model [9]. Note however, that in this work the Intelligent Driver Model (IDM) [10] replaces the corresponding Gipps model, since the latter does not represent capacity drop phenomena realistically [11].

2.3.1 Gipps Model

The Gipps car-following model, is formulated as two independent sub-models, one for acceleration and one for deceleration. Both equations output the speed of the vehicle at given time t, in terms of it's speed at the previous step.

The acceleration equation that describes the Gipps car-following model is the following:

$$v_n^{acc}(t+\tau) = v_n(t) + 2.5 a_n \tau \left(1 - \frac{v_{\text{n}}(t)}{v_n^d}\right) \sqrt{0.025 + \frac{v_{\text{n}}(t)}{v_n^d}} \tag{2.1}$$

The deceleration equation that describes the Gipps car-following model is the following:

$$v_n^{dec}(t+\tau) = -\tau d_n + \sqrt{\tau^2 d_n^2 + d_n \left\{ 2\left[x_{n-1}(t) - x_n(t) - S_{n-1}\right] - \tau v_n(t) + \frac{v_{n-1}(t)^2}{d'_{n-1}} \right\}} \quad (2.2)$$

From the equations above τ is the reaction time where $v_n(t)$ and $v_{n-1}(t-1)$ are, respectively, the speeds of vehicles n (follower) and n-1 (leader) at given time t, v_n^d and a_n are respectively the follower's desired speed and maximum acceleration, d_n and d'_{n-1} are respectively the most severe braking that the follower wishes to undertake and his estimate of the leader's most severe braking capability ($d_n > 0$ and $d'_{n-1} > 0$), $x_{n-1}(t)$ and $x_n(t)$ are respectively the leader's and the follower's longitudinal positions at time t, and S_{n-1} is the "leader's effective length", that is, the leader's real length L_{n-1} added to the follower's desired inter-vehicle spacing at stop s_{n-1} (between front and rear bumpers).

2.3.2 IDM Model

The IDM car-following model is a time and space continuous car-following model, formulated as an ordinary differential equation. The model describes the dynamics of a single vehicle, e.g. the position and the velocity of the vehicle. The velocity difference $\Delta v(t)$, the gap s(t) and the actual velocity $v(t)$, are the main model parameters.

Therefore, the acceleration equation that describes the IDM car-following model follows:

$$\dot{v}(s, v, \Delta v) = a\left[1 - (\frac{v}{v_o})^4 - (\frac{s^*(v, \Delta v)}{s})^2\right] \quad (2.3)$$

The equation consists of two parts. The $\dot{v}_{free}(v) = a\left[1 - (\frac{v}{v_o})^4\right]$ which defines the speed based on the maximum desired speed v_o on a free road with the parameter a being the maximum acceleration and the $\dot{v}_{brake}(s, v, \Delta v) = - a(s^*(v, \Delta v)/s)^2$ which dominates if the current gap $s(t)$ to the preceding vehicle becomes smaller than the desired minimum gap defined by the following Equation:

$$s^*(v, \Delta v) = s_o + vT + \frac{v\Delta v}{2\sqrt{ab}}, \tag{2.4}$$

where b is the comfortable deceleration, s_o is the minimum bumper-to-bumper distance to the front vehicle and T is the desired safety time headway when following other vehicles. The minimum distance s_o in congested traffic is significant for low velocities only. The dominating term of Equation (2.3) in stationary traffic is vT which corresponds to following the leading vehicle with a constant desired (safety) time gap T. The last term is only active in non-stationary traffic and implements an "intelligent" driving behavior including a braking strategy that, in nearly all situations, limits braking decelerations to the comfortable deceleration b. Note, however, that IDM brakes stronger than b if the gap becomes too small. This braking strategy makes IDM collision-free. All IDM parameters e.g. v_o, T, s_o, a and b are defined by positive values [8].

2.4   Lane Changing Model

The transfer of a vehicle from one lane to next adjacent lane is defined as lane change. Lane changing has a significant impact on traffic flow. Lane changing models are the

11

most important component of a microscopic traffic simulator, which is the tool of choice for a wide range of traffic-related applications at the operational level. Modeling the behaviour of a vehicle within its present lane is relatively straightforward, considering only the speed and location of the preceding vehicle. Lane changing, however, is more complex, because the decision of the driver to change lane is depended on numerous factors, incidents that sometimes may conflict to each other [12].

AIMSUN microscopic simulator uses by default the Gipps lane-changing model [13]. The fact is, that this model cannot capture the merging behavior in a critical flow regime [14]. The need for improvement, has led us to replace it with some heuristic rules [15].

2.4.1 Gipps Model

Lane changing manoeuvres and especially lane changing manoeuvres of vehicles at the proximity of a bottleneck have a high level of interaction among all vehicle movements. AIMSUN uses a development of the Gipps lane changing model. The lane-changing process is modelled as a decision making process that emulates the driver's behaviour when he or she is considering whether to change lanes (as in the case of turning manoeuvres determined by the route), the desirability of the lane change (e.g. to overtake a slow vehicle) and the feasibility conditions for the lane change. A lane change also depends on the location of the vehicle on the road network. To achieve a more accurate representation of the driver's behaviour in the decision-making process, Aimsun considers three different zones inside a section, each of which corresponds to a different

lane-changing motivation, based on the classification of the location of the vehicle into one of those three zones.

The zones are defined as follows:

- **Zone 1:** when a vehicle enters the zone, it only considers lane changing desirability to reach its desired speed. Also, lane changing decisions are mainly governed by the traffic conditions of the lanes involved, e.g. speed of the follower, speed of the leader, gap acceptance.

- **Zone 2:** when a vehicle enters the zone, is constantly looking for an acceptable gap and may try to accept it without affecting the driving behaviour of the vehicles in the adjacent lanes. This zone is characterized as the intermediate zone.

- **Zone 3:** this zone is the last and nearest zone to the next turning point. When a vehicle enters the zone, is forced to reach it's desired lane, with a possibility of reducing it's speed if necessary. Moreover, drivers being at the adjacent lanes may also modify their driving behaviour to create a gap that is sufficiently large for the lane-changing vehicle [16].

2.4.2 Heuristic Rules

Lane-drop region by definition, is a part of a network where the number of lanes provided for through traffic are decreased. This part is characterized as a bottleneck location. Lane changes in the immediate proximity of a bottleneck are not avoided, causing retarded merging driving behaviour. As it is observed, the Gipps lane-changing model

developed in Aimsun Microscopic Simulator results non realistic merging behavior. Due to this fact, the model is replaced with some heuristic rules at the bottleneck area, so as to achieve a more realistic approach on the way the drivers merge to the main network from the lane-drop region.
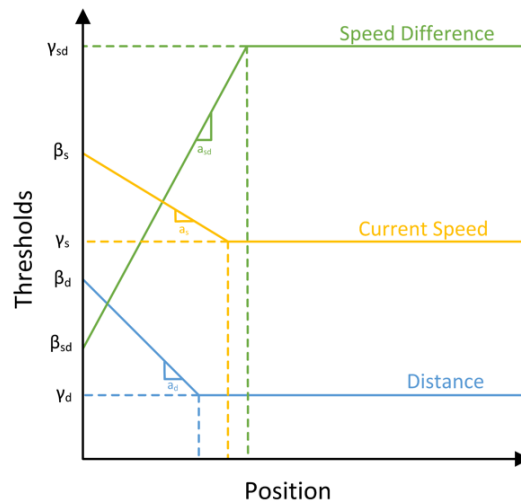
Figure 2.1: Graphical representation of the heuristic rules used for replacing the Gipps lane-changing model. The rules are based on the current speed of the vehicle, distance from the end of the segment and difference between speeds.

The concept of the heuristic rules used for replacing the Gipps lane-changing model consist of a set of inequality conditions based on three primary variables [15, 17].

The variables are defined as follows:

- current speed: speed of the vehicle at given time t.

- relative speed: speed with respect to the target-lane vehicles.

- available gap: acceptable gap in the target lane for accomplishing a safe transfer from one lane to another

In particular, linear functions of the vehicle's current position determine the threshold values of those variables, as illustrated in Figure 2.1 where two regimes can be noticed. In the first region the threshold values are linearly dependent on the position of the vehicle while in the second regime the threshold values remain constant. Note that in the first region the current speed and the distance thresholds are decreasing while the threshold of the relative speed difference is increasing with respect to the position of the vehicle. The current state of the vehicle needs to have greater values of current speed and distance than the threshold values of these linear rules while the speed difference has to be lower than the respective threshold value. Once these conditions are simultaneously satisfied then the vehicle is mandated to move to another lane. As it can be observed, the conditions are easier to be satisfied as the vehicle moves further downstream where the threshold values are relaxed [18]. Perraki et.al (2016) proposed a calibration procedure of parameters i.e. slope, initial and final value of the linear equations in order to determine these heuristic rules.

CHAPTER 3

Control Strategies

Longer travel times, lower speeds, long queues in the network, are a few of the immediate consequences of traffic jams on motorways. Since the existing motorways are underutilised especially in periods of high demand due to congestion, one possible solution is the construction of wider road infrastructures, with an enormous economical cost and significant environmental consequences [2]. Another more efficient way to overcome this situation, is the development and implementation of proper traffic control strategies with the aim of reducing traffic congestion and increasing the overall capacity of traffic networks.

3.1 Introduction

Consider a hypothetical motorway stretch featuring a lane-drop bottleneck (Figure 3.1). As long as the arriving demand q_{in} upstream of the bottleneck is less than or equal to the capacity q_{cap}^{down} downstream of the bottleneck, no problem occurs. Congestion

is typically initiated at bottleneck locations, when the arriving demand q_{in} is higher than the bottleneck capacity q_{cap}^{down} ($q_{in} > q_{cap}^{down}$). Thus the bottleneck is activated and congestion spills back covering sections upstream of the bottleneck location as long as the upstream arriving flow is sufficiently high.
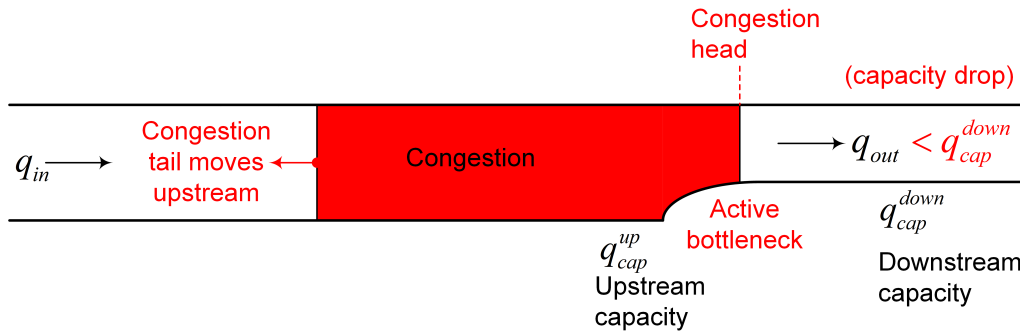
Figure 3.1: Lane drop bottleneck notion

The congestion forming at an active bottleneck has two kinds of detrimental effects on the motorway capacity and throughput [19]. These detrimental effects are:

- **Capacity drop (CD) at the congestion head:** Bottleneck activation leads to a speed breakdown upstream of the bottleneck location. As a result, different vehicle accelerations from lower (within the congestion) to higher speeds (downstream of the bottleneck), are deemed to lead to a capacity drop which breeds a reduction in the mainstream flow and consequently an active bottleneck outflow q_{out} that may be $5\% - 15\%$ lower than the nominal capacity q_{cap}^{down}.

- **Blocking of off-ramps (BOR):** Congestion tail is covering related off-ramps, as it moves upstream of the bottleneck location over several kilometers on the mainstream. As a result, the off-ramp flow drops as well, and vehicles bound for the

off-ramps are getting trapped within the congestion accelerating its spillback further upstream.

Note that the BOR effect is independent of the CD effect and leads to an additional reduction of the freeway throughput, i.e. it reflects an additional source of infrastructure degradation [19]. To avoid or delay the activation of a bottleneck and the related capacity drop phenomenon, we investigate the first strategy Mainstream Traffic Flow Control using Variable Speed Limits.

3.2 Variable Speed Limits

VSL displayed on road-side variable message signs (VMSs) in response to prevailing traffic conditions is an increasingly popular motorway traffic control measure [20]. A main targeted impact of VSLs is enhanced traffic safety as a result of the homogenisation of speeds of individual vehicles and of the mean speeds of different motorway lanes which reduce the accident risk [20]. In this work we investigate the proper use of VSL to connected vehicles that may directly receive the value of the speed limit that is delivered by the control strategy, according to their current location in the network, and it is expected that, for sufficient penetration of equipped vehicles, this will be sufficient to impose the speed limit to non-equipped vehicles as well; hence, no VMS-gantries would be necessary.

3.2.1 Methodology

The basic idea of Mainstream Traffic Flow Control (MTFC) is to enable the mainstream traffic flow at areas with particular infrastructure i.e. lane-drop bottlenecks, to take values ordered by an appropriate control strategy in order to establish optimal traffic conditions for any appearing demand [21]. The MTFC concept used in this thesis is illustrated in Figure 3.2.
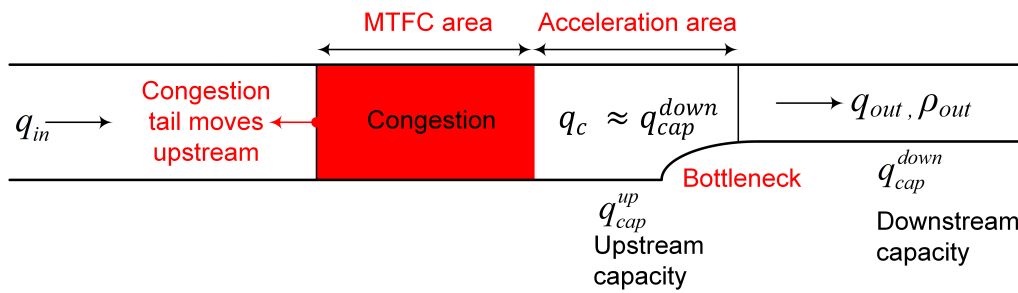
Figure 3.2: MTFC application

MTFC actions using Variable Speed Limits (VSL) as actuators are employed in order to regulate the mainstream flow upstream of the bottleneck location. When the arriving demand q_{in} is less than the q_{cap}^{down}, bottleneck is not activated; hence no MTFC actions are needed. On the other hand, when the arriving demand exceeds the nomical capacity of the bottleneck q_{cap}^{down}, discharge flow is lower due to the capacity drop phenomenon that calls for the necessity of MTFC actions. Once MTFC actions are employed, a controlled congestion is formed further upstream of the bottleneck location leaving enough space for the vehicles to accelerate within the acceleration area and hence increase the outflow to be equal to the nominal capacity of the bottleneck $q_c \approx q_{cap}^{down}$.

Furthermore, to avoid abrupt decelerations as soon as vehicles approach the MTFC area, VSL is also applied further upstream to ensure a controlled reduction of speed and a safer approach at the MTFC area. Note that, the controlled congestion is significantly reduced in space and time compared to the congestion created in the no-control case, with higher internal speeds due to the increased outflow values. Finally, less blocking of off-ramps leads to further improvements on the freeway.

3.2.2 Feedback Control Strategy Design

A Proportional - Integral (PI) feedback regulator is employed for MTFC, keeping the bottleneck density ρ close to the selected set-point $\hat{\rho}$ using real time measurements (or estimates) of ρ [22]. The set-point is typically selected around the critical density value, at which capacity flow is achieved at the bottleneck location. The equation that describes the PI-type regulator reads:

$$vsl(k) = vsl(k-1) + K_I(\hat{\rho} - \rho(k)) + K_P(\rho(k-1) - \rho(k)) \tag{3.1}$$

with $k(=1,2,3,...)$ defined as the discrete time index. Proportional and Integral gains of the controller are denoted by K_P and K_I, respectively. The $vsl(k)$ value delivered by the control strategy is truncated to remain within a range of admissible VSL values $[vsl_{min}, vsl_{max}]$ and is used at the next time period as $vsl(k-1)$ in order to avoid the windup phenomenon [23]. Upstream of the MTFC application area (where VSL is active) there are safety areas where speed limits are also applied to ensure a smooth

reduction of speed and a safer vehicle approach to the application area. Furthermore, downstream of the application area, an acceleration area follows in order to allow a quick recovery of higher speeds that maximize the bottleneck throughput.

Some VSL practical implementation aspects are then taken into account. VSL can only take predefined discrete values (e.g. 90, 80, 70,... km/h). Furthermore, the difference between two consecutive VSL values received by connected vehicles in a segment of the freeway is limited (e.g. to ± 10 km/h), so as to avoid abrupt speed changes. Also, the difference between two VSL values at consecutive segments at the same control period is limited (e.g. to 10 km/h), as often required in practice, in order to achieve a safe approach of vehicles within the safety areas.

3.3 Lane Change Control Actions

In the following decade, vehicle automation and communication systems (VACS) are expected to revolutionize the features and capabilities of individual vehicles and hence contribute to improve traffic control performance. Of the wide range of potentially introduced VACS, some may be exploited to interfere with driving behavior via recommending, supporting, or even executing appropriately designed traffic control tasks [24]. However, the uncertainty about the future development of VACS calls for the design of control strategies that are robust with respect to the different system types, as well as to their penetration rate. A promising new feature that can be exploited for traffic management is lane-changing control [17].

21

3.3.1 Introduction

LCC is a promising new strategy that can be exploited for traffic management [17, 25]. The basic goal of lane-changing control is to achieve a desired distribution of vehicles among the lanes in the immediate proximity of a bottleneck, so as to exploit the capacity of each and every lane, thus increasing the overall (cross-lane) capacity. To this end, a linear state-feedback control law, resulting from an appropriate linear-quadratic regulator problem formulation, is developed. The considered system under control comprises a number of interacting segment-lanes upstream of the bottleneck; while the feedback control law computes adequate lateral (lane-changing) flows for each segment-lane, thus enabling an opportune, pre-specified distribution of traffic flow among the lanes. More specifically, the feedback control law uses real-time measurements (or estimates) of the state of the system, i.e. of all segment-lane densities, and is targeting appropriate pre-specified set-points of lane-based traffic densities.

3.3.2 Multi-lane traffic flow model

In this thesis a multi-lane macroscopic traffic flow model is used, as described in [17, 25] which is proved efficient for optimal control problem formulations due to it's simple mathematical form and traffic dynamics aspects. Consider a multi-lane motorway stretch as presented at Figure 3.3 that is subdivided into $i = 1, ... , N$ segments of length Li, while each segment is composed of $j = m_i, ... , M_i$ lanes, where m_i and M_i are the minimum and maximum indexes of lanes for segment i.
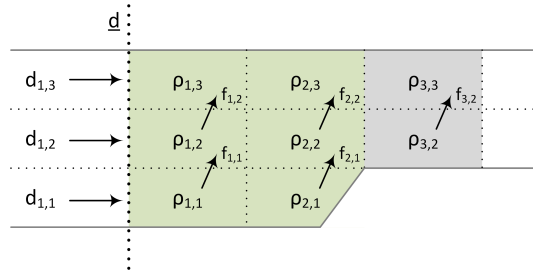
Figure 3.3: Model formulation

Each segment *i* is composed of M_i - m_i *+1* cells; while each motorway cell is indexed by *(i,j)*. According to this definition, the total number of cells from the origin to segment *i* is $H_i = \sum_{r=1}^{i}(M_r - m_r + 1)$ and the total number of cells for the whole stretch is $\overline{H} = H_N$. It is assumed that *j = 1* corresponds to the right most lane of the motorway. For example, looking at the hypothetical motorway stretch depicted in Figure 3.3, $m_i = 1$ and $M_i = 3$ for segments with index *i = 1, 2* while $m_i = 2$ and $M_i = 3$ for segment with index *i = 3*. The model is formulated in discrete time, considering the discrete time step *T*, indexed by *k = 0, 1,. . . . ,* where the time is *t =kT*.
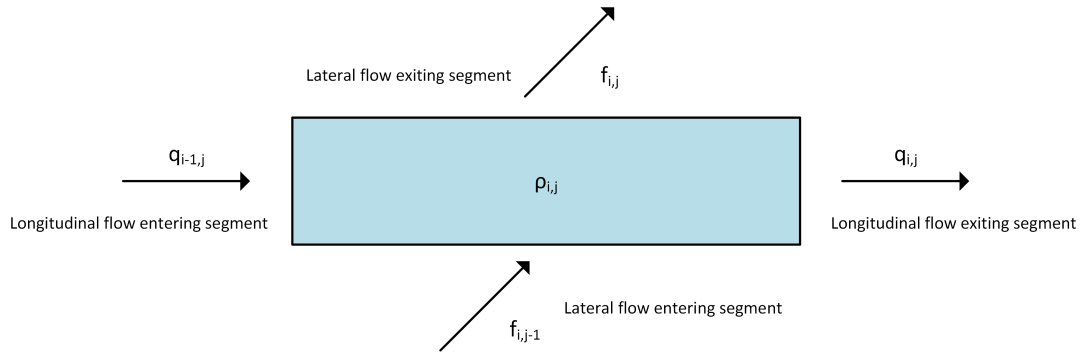
Figure 3.4: Segment-lane formulation

Each cell *(i,j)* as illustrated in Figure 3.4 is characterized by traffic density $\rho_{i,j}(k)$, which is dynamically evolved following the conservation equation:

$$\rho_{i,j}(k+1) = \rho_{i,j}(k) + \frac{T}{L_i}\left[q_{i-1,j}(k) - q_{i,j}(k)\right] + \frac{T}{L_i}\left[f_{i,j-1}(k) - f_{i,j}(k)\right] + \frac{T}{L_i}d_{i,j}(k) \quad (3.2)$$

where:

Variable	Unit	Definition
$\rho_{i,j}(k)$	[veh/km]	the number of vehicles travelling in each segment - lane divided by the segment length L_i
$q_{i,j}(k)$	[veh/h]	the number of vehicles leaving segment i and entering segment $i+1$, remaining at lane j during time interval $(k, k+1]$
$f_{i,j}(k)$	[veh/h]	the number of vehicles moving from lane j to lane $j+1$ during time interval $(k, k+1]$
$d_{i,j}(k)$	[veh/h]	external flow entering network in each segment - lane during time interval $(k, k+1]$

Table 3.1: Segment - lane entities characterized by variables

Depending on the network topology, some terms of equation (3.2) may not be present. Particularly, the inflow $q_{i-1,j}(k)$ does not exist for the first segment of the network; the outflow $q_{i,j}(k)$ does not exist for the last segment before a lane drop, while the lateral flow term $f_{i,j}(k)$ exists only for $m_i \leq j < M_i$. Note that in order to ensure numerical stability, the time step T must respect Courant–Friedrichs–Lewy CFL condition:

$$T \leq min_{i,j} \frac{L_i}{v_{i,j}^{max}} \tag{3.3}$$

where $v_{i,j}^{max}$ is the maximum speed allowed in each cell *(i,j)* and L_i is the length of each segment. Note that, the lateral flow term $f_{i,j}(k)$ is considered only in one direction, from the right to left lanes based on the network topology illustrated in Figure 3.4. Therefore, the optimal control problem formulation is computationally faster, since lateral flows are treated as control inputs.

Considering and replacing the well-known relationship

$$q_{i,j}(k) = \rho_{ij}(k)v_{i,j}(k)$$

into the conservation law equation (3.2), a further correlation among the variables is obtained as follows:

$$\rho_{i,j}(k+1) = \frac{T}{L_i}v_{i-1,j}(k)\rho_{i-1,j}(k) + \left[1 - \frac{T}{L_i}v_{i,j}(k)\right]\rho_{i,j}(k)+ \tag{3.4}$$

$$\frac{T}{L_i}\left[f_{i,j-1}(k) - f_{i,j}(k)\right] + \frac{T}{L_i}d_{ij}(k)$$

treating our system as a **Linear Parameter Varying** (LPV) system in the form:

$$x(k+1) = A(k)x(k) + Bu(k) + d(k) \tag{3.5}$$

We denote as

$$\underline{x} = \begin{bmatrix} \rho_{1,m_1}...\rho_{1,M_1} & \rho_{2,m_2}...\rho_{N,M_N} \end{bmatrix}^T \in \mathbb{R}^{\overline{H}} \tag{3.6}$$

$$\underline{u} = \begin{bmatrix} f_{1,m_1}...f_{1,(M_1-1)} & f_{2,m_2}...f_{N,(M_N-1)} \end{bmatrix}^T \in \mathbb{R}^{\overline{F}} \tag{3.7}$$

$$\underline{d} = \begin{bmatrix} \dfrac{T}{L_1}d_{1,m_1}...\dfrac{T}{L_1}d_{1,M_1} & \dfrac{T}{L_2}d_{2,m_2}...\dfrac{T}{L_N}d_{N,M_N} \end{bmatrix}^T \in \mathbb{R}^{\overline{H}} \tag{3.8}$$

where:

Variable	Unit	Definition
$\underline{x}(k)$	[veh/km]	density for each motorway cell (i,j) during time interval $(k, k+1]$
$\underline{u}(k)$	[veh/h]	lateral flows treated as control inputs during time interval $(k, k+1]$

Table 3.2: Linear Parameter Varying System characterized by variables

Matrix $A(k)$ representing the connection between pairs of subsequent cells connected

by a longitudinal flow $q_{i,j}(k)$ is composed of elements:

$$
a_{r,s} = \begin{cases}
1, & \text{if } r = s \text{ and } (j < m_{i+1} \text{ or } j > M_{i+1}) \\[2em]
1 - \frac{T}{L_i} v_{i,j}(k), & \text{if } r = s \text{ and } (i = N \text{ or } m_{i+1} \leq j \leq M_{i+1}) \\[2em]
\frac{T}{L_i} v_{i-1,j}(k), & \text{if } r > H_1 \text{ and } s = r - M_{i-1} + m_i - 1 \\[2em]
0, & \text{otherwise}
\end{cases}
$$

Also matrix B reflecting the connection of adjacent cells connected by lateral flows $f_{i,j}(k)$, is composed of elements:

$$
b_{r,s} = \begin{cases}
\frac{T}{L_i}, & \text{if } j > m_i \text{ and } s = r - i \\[2em]
-\frac{T}{L_i}, & \text{if } j < M_i \text{ and } s = r - i + 1 \\[2em]
0, & \text{otherwise}
\end{cases}
$$

where $r = H_{i-1} + j + m_i + 1$.

Assuming that the inflow arriving upstream of the bottleneck location is not exceeding the maximum capacity of the bottleneck, and that any formation of congestion can be avoided, our system can be treated as a Linear Time Invariant (LTI) system. In free flow conditions, it is assumed that speed $v_{i,j}(k)$ in all cells (i,j) remains constant and equal to free speed v_{free} $(v_{i,j}(k) \equiv v_{free})$. Thus, matrix $A(k)$ is now treated as a constant matrix A. Also, external flow $d_{i,j}(k)$ is assumed constant due to slow variations expected for its values. Based on this aspect, the LTI system reads:

$$\underline{x}(k+1) = A\underline{x}(k) + B\underline{u}(k) + \underline{d} \tag{3.9}$$

3.3.3 Quadratic Cost Function

For the purpose of maintaining the density at the bottleneck area below its critical value and thus avoid exceeding the nominal capacity of the bottleneck, a quadratic cost function defined over an infinite time horizon follows [25]:

$$J = \sum_{k=0}^{\infty} \left\{ \sum_i \sum_j \alpha_{i,j} \left[\rho_{i,j}(k) - \hat{\rho}_{i,j} \right]^2 + \sum_{i=0}^{N} \sum_{j=m_i}^{M_i-1} \left[f_{i,j}(k) \right]^2 \right\} \tag{3.10}$$

The first term accounts for the difference between some densities and pre-specified (constant) set-point values. The second term aims at maintaining small control inputs, i.e., small lateral flows.

The matrix form of the function also follows:

$$J = \sum_{k=0}^{\infty} \left\{ \left[C\underline{x}(k) - \hat{\underline{y}} \right]^T Q \left[C\underline{x}(k) - \hat{\underline{y}} \right] + \underline{u}^T \underline{u}(k) \right\} \tag{3.11}$$

where:

C = matrix, reflects the cells that are tracked.

Q = weighting matrix, associated to the magnitude of the state tracking error

$\hat{\underline{y}} \in \mathbb{R}^{\overline{Y}}$ is a vector containing the $\overline{Y}$ selected desired set-point density values at the bottleneck area.

Note that $Q = Q^T$ is a positive definite matrix and matrix C is composed of elemenets $c_{r,s}$ ($1 \leq r \leq \overline{Y}$ rows and $1 \leq s \leq \overline{H}$ columns):

$$c_{r,s} = \begin{cases} 1, & \text{for cells that are tracked (downstream of the lane-drop area)} \\ 0, & \text{otherwise} \end{cases}$$

An appropriate solution to the problem considering the minimization of the quadratic cost function (3.11) is given through a Linear Quadratic Regulator (LQR). A linear state feedback-feedforward control law is the optimal solution to the (LQR) problem. In order to ensure a stabilizing feedback-feedforward control law, our system must be at least stabilisable and detectable [25].

3.3.4 Stabilisability-Detectability

Initially a control system is characterized by it's state variables. In the majority of cases, a system may have uncontrollable state variables; thus, the system is not stabilisable. It is defined that, a system is stabilisable when all uncontrolled state variables can be made to have stable dynamics. For the system described at (3.9), we draw our attention to matrix A. To address stabilisability, we can see that matrix A, is a lower triangular matrix implying that it's eigenvalues λ are equal to the elements in the main diagonal. Since speed v is always positive the modes related to segments for which another downstream segment exists are always stable (implying that its eigenvalues $|\lambda| < 1$ are less equal to one), while the modes related to segments without any other segment downstream (i.e., at a lane-drop) are marginally stable ($\lambda = 1$) [25]. According to the Hautus-test [26], the system is stabilisable if, for each unstable (or marginally stable) mode, relation

$$rank[(\lambda I - A) \quad B] = \bar{H} \tag{3.12}$$

is satisfied. This implies that, to guarantee that the pair (A,B) is stabilisable, B must have more linearly independent columns than the number of non-stable $|\lambda| \geq 1$ modes, that is, for each lane dropping, there must be at least one controlled lane-changing, which is trivially satisfied for the defined network structure [25]. For the detectability of our system we consider the following pair: $(A, C^{T}QC)$. Matrix Q is a positive matrix; thus detectability of the pair (A, C) is equivalent [27]. According to Hautus-test, the system

30

is detectable if, for each unstable (or marginally stable) mode, relation

$$rank \begin{bmatrix} (\lambda I - A) \\ C \end{bmatrix} = \bar{H} \tag{3.13}$$

is satisfied. In our case, this is verified in case C has at least a non-zero element in each column corresponding to $\lambda = 1$, which implies controlling the density of each cell that does not have any other cell downstream. This requires the definition of an arbitrary setpoint for the density in this cell, which is, for practical reasons, undesirable. To account for this issue, we propose to place an additional dummy cell immediately downstream of each lane-drop, imposing it, with an appropriate high penalty weight $\alpha_{i,j}$ to have a density equal to zero. Note that, in the described case, the system is also observable [25].

3.3.5 Linear State Feedback-Feedforward Control Law

The linear feedback-feedforward control law is given by:

$$\underline{u}^*(k) = -K\underline{x}(k) + \underline{u}_{ff} \tag{3.14}$$

considering as:

$$K = (R + B^T PB)^{-1} B^T PA \tag{3.15}$$

$$P = C^T QC + A^T PA - A^T PB(R + B^T PB)^{-1} B^T PA \tag{3.16}$$

$$\underline{u}_{ff} = (R + B^T PB)^{-1} B^T F(C^T Q\hat{\underline{y}} - P\underline{d}) \tag{3.17}$$

$$F = (I - (A - BK)^T)^{-1} \tag{3.18}$$

Note that the feedback gain matrix K is calculated via (3.15) only once offline (non-time varying) after solving the Ricatti equation (3.16) iteratively starting from $P = I$. Subsequently, equation (3.17) with F from (3.18), represents the feedforward term that may be calculated offline. However, for practical implementation, one may measure the external flow $\underline{d}$, in which case the feedforward term becomes time varying (online), with equations (3.14, 3.17) rewritten as:

$$\underline{u}^*(k) = -K\underline{x}(k) + \underline{u}_{ff}(k) \tag{3.19}$$

$$\underline{u}_{ff}(k) = (I + B^T PB)^{-1}B^T F(C^T Q\hat{\underline{y}} - P\underline{d}(k)) \tag{3.20}$$

Note that, optimal gain K and the Riccati equation can be found in [28].

CHAPTER 4

Application and Results

4.1 Network Description

The infrastructure layout for the investigation of the proposed strategies [17], [22], [25] was developed and tested using AIMSUN Microscopic Simulator (Advanced Interactive Microscopic Simulator for Urban and Non-urban Networks). AIMSUN includes the AAPI and the microSDK tools, that allow the modification of a simulation as it runs and the replacement of the current models used by the simulator. The MTFC and the LCC strategy were implemented using the AAPI tool; while on the other hand the microSDK tool was used to overwrite Aimsun's default behavioral models.

A hypothetical freeway stretch featuring a lane-drop bottleneck is considered in this paper for investigating the integrated use of the two feedback control strategies. Four scenarios are defined (no-contol scenario, variable speed limits scenario, lane changing control scenario, integrated control scenario).

The freeway stretch illustrated in Figure 4.1 consists of 10 segments of 0.5 km each, resulting in a total 5.0 km length. The biggest part of the network features 3 lanes starting from the entrance until reaching the 4.0 kilometer of the freeway where the right-most lane (lane 1) drops and then, the last kilometer has 2 lanes. Lane 2 is the middle lane and lane 3 is the left lane of the network (fast lane). When no VSL values are applied, the nominal speed limit is 100 km/h for all sections except for the two consecutive segments upstream of the bottleneck in where the speed limit is set to 80 km/h.
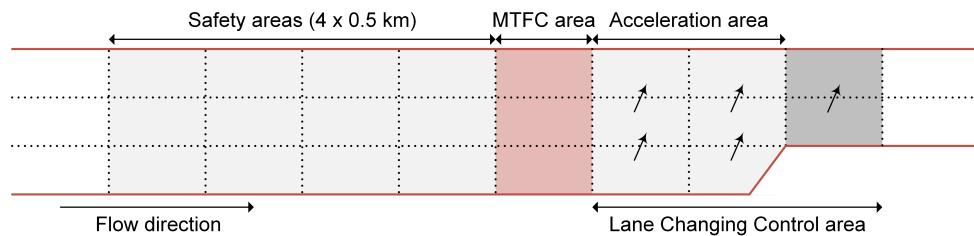
Figure 4.1: Infrastructure and strategies

Ten replications are conducted for each scenario for a simulation horizon of $T = 60$ min. Each replication has the same average demand profile and the same mean values for all vehicle-related parameters. For each scenario, one replication close to the average of the ten replications is selected for presentation in the following sections. The traffic demand profile for one of the replications is depicted in Figure 4.2. It can be observed that the demand is increasing for about 10 minutes reaching values ($\sim$4200 veh/h) well above the capacity of the bottleneck (3600 veh/h). The demand remains high for about 15 minutes and then it is decreasing and is staying at low values so as to allow for free

34

flowing conditions at the end of the simulation horizon for all scenarios considered and, as a result, allow also the comparison of performance indexes between different scenarios.
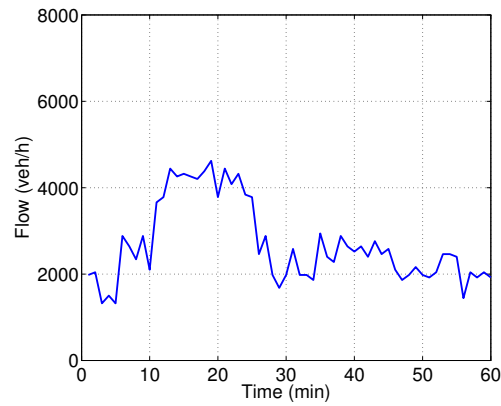
Figure 4.2: Traffic demand profile

4.1.1 Parameters Setup

In the majority of cases, without calibration, a model will not accurately predict traffic state conditions. Calibration is considered as a key part for the reliability of the simulator and the experiments that one can conduct via these tools. The main aspect of tuning the model parameters is to improve its ability to reproduce observed local driver behavior and traffic performance characteristics. In this thesis the calibration process was based on [18], using a trial and error process so as to achieve a realistic driving behavior upstream of the bottleneck area.

The calibrated parameters are presented in the following table:

Papameter	Mean Value	Deviation	Min Value	Max Value
Max acceleration (m/s^2)	2.46	0.20	1.87	3.07
Normal deceleration (m/s^2)	2.81	0.20	2.21	3.41
Minimum Headway (sec)	0.88	0.10	0.58	1.18
Min distance vehicle (m)	3.00	0.20	2.20	4.00
Max desired speed (km/h)	110.00	10.00	80.00	150.00
Max give-way time (sec)	12.97	2.64	7.69	18.25

Table 4.1: Calibrated Aimsun parameters

Additionally, other parameters used by the microsimulator were tuned manually after the calibration process of the most crucial parameters illustrated above.

These parameters are presented in the following table:

Papameter	Calibrated Value
Reaction time at stop (sec)	1.1
Percentage Overtake $(\%)$	90
Percentage Recover $(\%)$	95
Percentage for staying in overtaking $(\%)$	10
Percentage for imprudent lane-changing $(\%)$	40

Table 4.2: Other parameters

4.1.2 Parameters Description

- Maximum acceleration: This is the maximum acceleration, in (m/s^2), that the vehicle can achieve under any circumstances and is used in the proposed car-following model as the maximum acceleration a.

- Normal deceleration: This is the maximum deceleration, in (m/s^2), that the vehicle can use under normal conditions. It is used in the implemented car-following model as the comfortable deceleration variable b.

- Minimum Headway: This parameter ensures a minimum time headway between the leader and the follower. Concerning the IDM car-following model it is taken into account as the desired safety time headway.

- Minimum distance vehicle: This is the distance, in (m), that a vehicle keeps between itself and the preceding vehicle when stopped. It represents the minimum distance used in the car-following model formulation.

- Maximum desired speed: This is the maximum speed, in km/h, that a vehicle can travel at any point in the network. It is also used in the car-following model as the desired speed v_0.

- Maximum give-way time: When a vehicle has been at a standstill for more than this give-way time in (sec), it will become more aggressive and it will reduce the acceptance margins. This period is also used in the lane-changing model as the time that a vehicle accepts being at a standstill while waiting for a gap to be cre-

ated in the desired turning lane before giving up and continuing ahead.

- Reaction time at stop: This is the time it takes for a stopped vehicle to react to the acceleration of the vehicle in front.

- Percentage overtake: This parameter represents the percentage of the speed from which a vehicle decides to overtake.

- Percentage recover: It represents the percentage of the desired speed of a vehicle above which a vehicle may decide to get back into the slower lane.

- Percentage for Staying in overtaking: Percentage of vehicles that stay in a fast lane instead of recover a slower lane during an overtake manoeuvre.

- Percentage for Imprudent lane-changing: This parameter defines the percentage of vehicles that will apply a lane-changing with a non-safe gap.

4.1.3 Heuristic Rules Setup

Lane change is defined as the immediate transfer of a vehicle to an adjacent lane when needed. However, attempting to model the lane change behavior is more complicated. Specifically, when a vehicle is within a lane-drop lane, it needs to move to an adjacent lane before the lane drops. In this case, the lane change decision is based on vehicle's current position, current speed, relative speed with respect to the adjacent vehicles travelling in the mainstream and the available gap in the mainstream. These values are compared to the respective threshold values and if the conditions are satisfied, the vehicle safely changes lane. Note that, the applied rules used at the bottleneck area, were

calibrated from several tests within a calibration procedure described in detail in [18]. Figure 4.3 illustrates the aforementioned rules.
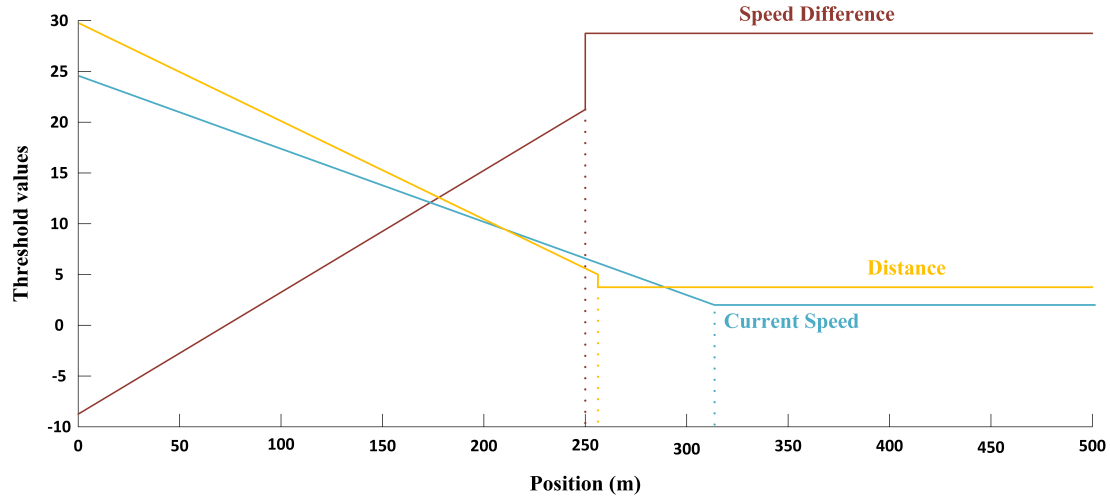

Figure 4.3: Threshold values applied at the bottleneck area

4.1.4 Mainstream Traffic Flow Control Application

For the MTFC scenario different penetration rates of 20%, 40%, 60%, 80%, 100% were investigated to test the effectiveness of the strategy. Density measurements are taken every $t = 60s$ from the detectors placed upstream of the bottleneck location. Also a desired critical density value is necessary for the VSL actuator to deliver the VSL value. The control strategy used in the VSL and the Integrated scenario, is employed to the mainstream illustrated in Figure 4.4 as follows :

- During the whole time-period $(k, k + 1]$ and for each one of the connected vehicles according to the penetration rate being in the acceleration area, a constant VSL value ("Capacity VSL") is delivered until the exit of the area.

Safety VSLs   Capacity VSL

DETECTORS

Congestion

Safety area 4   Safety area 3   Safety area 2   Safety area 1   MTFC area   Acceleration Area

VSL $\longleftarrow$ PI $\longleftarrow$ ρ_{out}
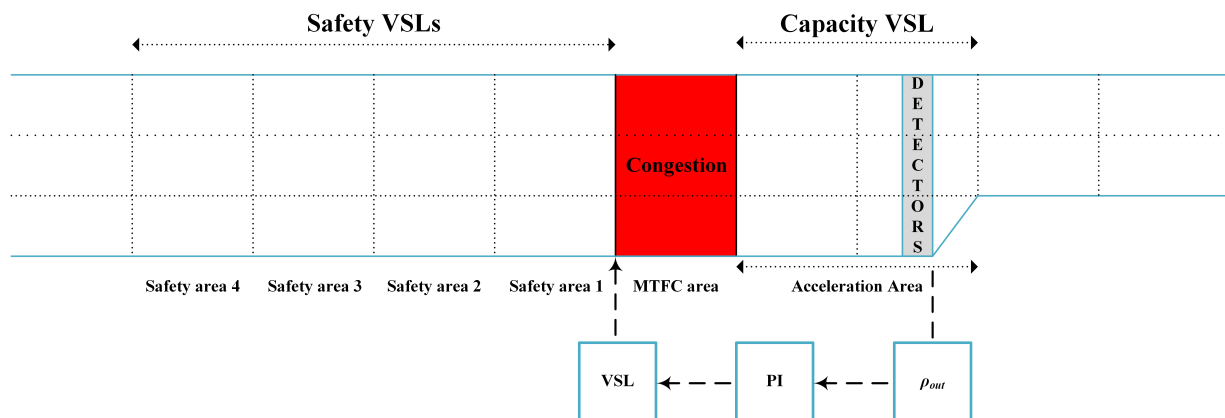
Figure 4.4: MTFC application

- Moreover "VSL" displaying the decision taken by the PI regulator (3.1) is delivered at the upstream end of the MTFC area.

- The most downstream detector station, close to the bottleneck, provides the real-time density estimates needed for the PI controller operation according to equation (3.1) [22].

- Finally, VSL values ("Safety VSLs") are delivered to all Safety areas starting from the most downstream Safety Area 1 and gradually increasing reaching Safety Area 4, to ensure that drivers will comfortably accept a recommended change of speed for safety conditions as they reach the MTFC area.

4.1.5   Lane Changing Control Application

For the Lane Change Control Scenario different penetration rates of 20%, 40%, 60%, 80%, 100% were investigated for the effectiveness of the strategy. The optimal lateral flows are computed for each segment-lane using real time measurements of the state
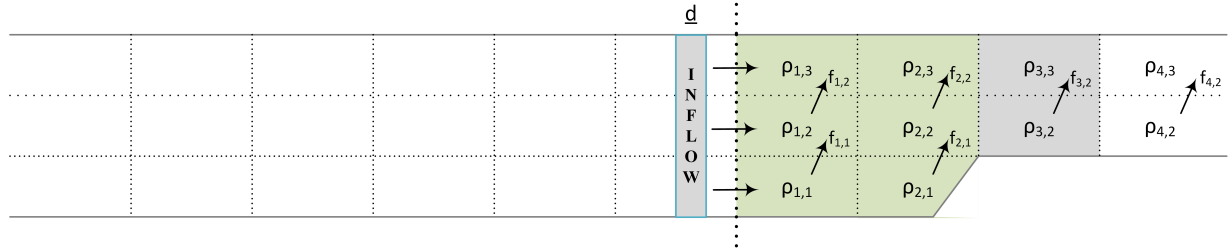
Figure 4.5: LCC application

of the system. Consequently, lateral flows are transformed to lane-changing orders and sent to an appropriate number of connected vehicles. It is assumed that for all connected vehicles, drivers are in full compliance with these advices. Specifically, appropriate LCC actions take place in segments 7 and 8 illustrated with green color at Figure 4.5 characterised by an equal penalty cost in order to facilitate the merging of vehicles upstream of the bottleneck location avoiding vehicles getting trapped at the drop lane.

4.2 Scenario Results

4.2.1 No Control Scenario

In the no-control scenario congestion starts at $t = 16$ min, as the arriving demand exceeds capacity, and lasts for about 30 min. It spills back covering several sections (1.5 km) upstream of the bottleneck location as depicted in the speed contour plot presented in Figure 4.6(a). Density trajectories are displayed in Figure 4.6(b) for each lane at the lane-drop area. After $t = 16$ min a quasi-simultaneous steep rise of density at lanes 2 and 3 indicates the corresponding drop of speeds and the formation of congestion at all lanes.

41

A capacity drop of about 14% of the nominal capacity of the bottleneck is observed in Figure 4.6(c). The outflows per lane, displayed in Figure 4.6(d), validate that lane 2 (blue trajectory) reaches its capacity ($\approx$ 2100 veh/h) and breaks down spreading congestion on lane 3 (red trajectory) that also breaks down at 1700 veh/h, i.e. before reaching its capacity. The average Total Travel Time (TTS) value for the no-control scenario is 223.3 veh·h.
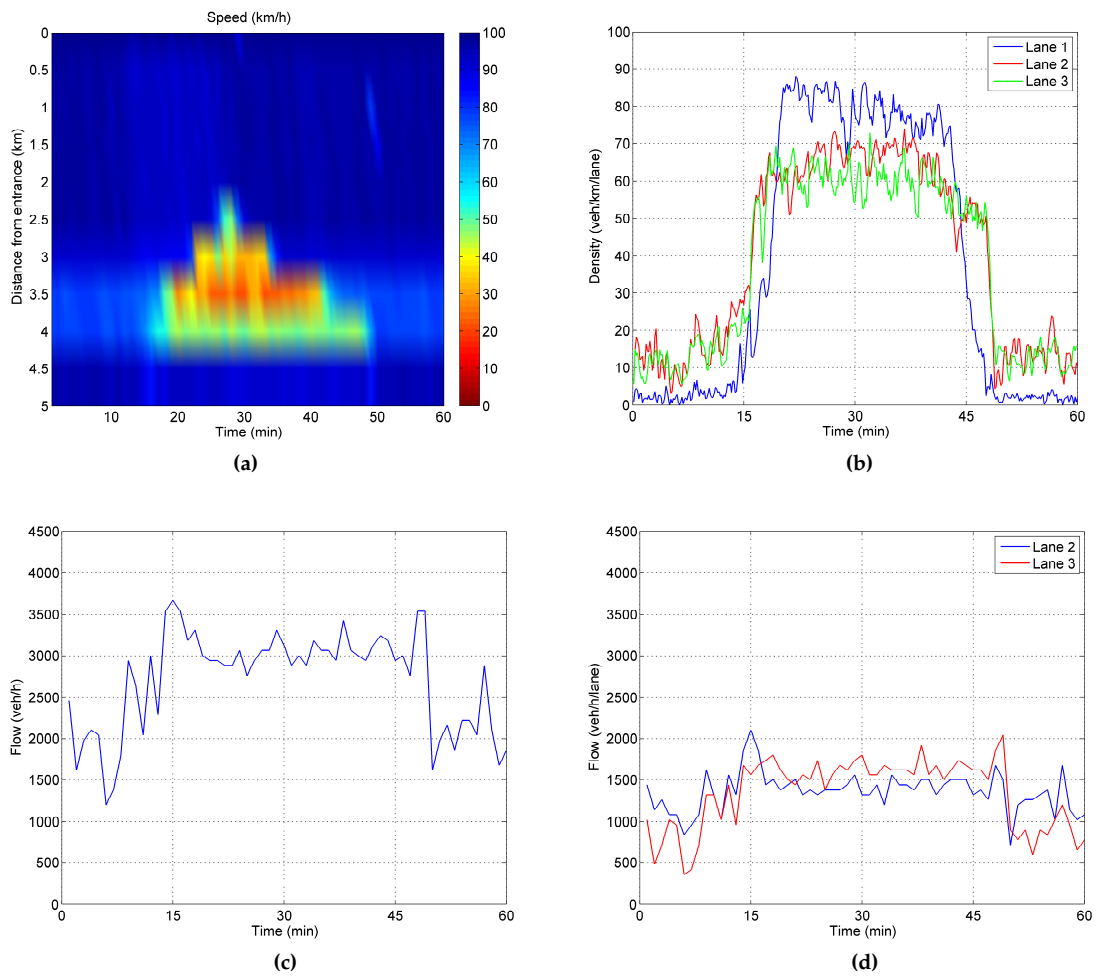
Figure 4.6: (a) Speed contour plot; (b) per lane density trajectories; (c) total outflow trajectory; and (d) per lane outflow trajectories at the lane-drop area for the no-control scenario

4.2.2 Variable Speed Limits Scenario

The main goal of MTFC is to regulate the mainstream flow upstream of the bottleneck, i.e. at the MTFC application area indicated in Figure 4.1, in order to maximise throughput. The penetration rate of connected vehicles that receive and apply VSL values is set to 20%. The speed contour plot resulting from MTFC application in the present investigation is presented in Figure 4.7(a).

(a)   **(b)**
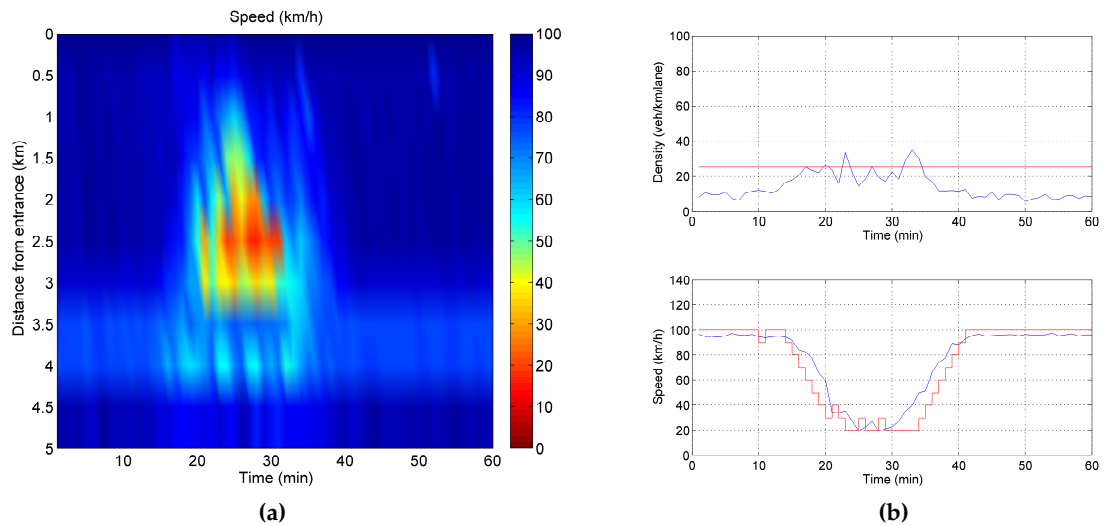
Figure 4.7: (a) Speed contour plot, (b) density measurements (blue line) at the bottleneck area (lane-drop area) with the corresponding critical density value (red line) and speed measurements at the MTFC application area with the corresponding speed limits (red line) for the VSL scenario

All actions are delivered by the PI controller (3.1) every 60 sec with a corresponding set-point equal to the critical density of 25 veh/km/lane, for which capacity flow is reached at the no-control scenario. Minimum and maximum values of VSL are set to 20 km/h and 100 km/h, respectively. No MTFC action is necessary up to $t = 16$

min. Then, as illustrated in Figure 4.7(b), density at the bottleneck area (lane-drop area) is increasing approaching the set-point. Therefore, VSL values ordered by (3.1) are gradually decreasing reaching the minimum admissible value (Figure 4.7(b)). All practical implementation aspects mentioned below (3.1) are applied.

Density at the bottleneck area (lane-drop area) is maintained around the set-point. Speed measurements at the MTFC application area demonstrate that even a penetration rate of 20% is sufficient to drive the average speed of all vehicles close to the ordered VSL value. Due to VSL actions, a controlled congestion is formed further upstream, that is reduced in space and time compared to the one formed in the no-control scenario. An improvement of 6.4% is achieved on the average TTS value.

As demonstrated in Figure 4.8, higher values in penetration rate of connected vehicles result into higher achieved improvement of the average TTS value approaching the value that corresponds to the case of VSL values displayed on VMS gantries, hence affecting the whole population of vehicles in the specific segments.
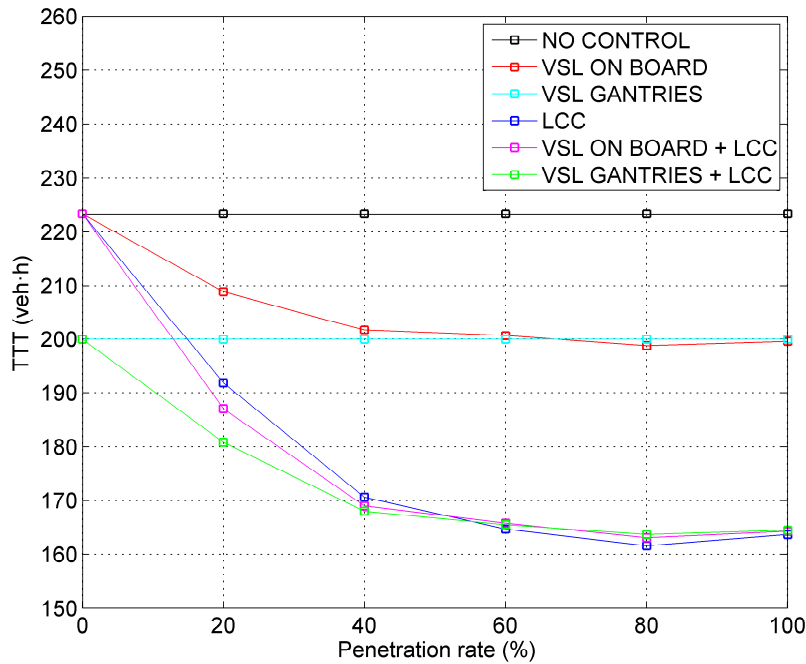
Figure 4.8: Average Total Travel Time (TTT) per penetration rate of connected vehicles for the no-control case and control cases

Further improvement is achieved in case 100% penetration rate of connected vehicles receive and apply VSL values. Specifically, the speed contour plot depicted in Figure 4.9(a) validates that no MTFC actions are taken until t=18min. During the period from t=18 min to t=40 min a controlled congestion is formed among the 1st and the 3rd kilometer while speed is gradually increasing backwards due to the variable speed limits applied at the Safety areas; leaving enough space for the vehicles to accelerate within the acceleration area among the upstream end of the 3rd and 4th kilometer. It is observed though, that congestion when employing MTFC actions is not avoided but is shorter in space and time for almost 8 min compared to the no-control scenario.
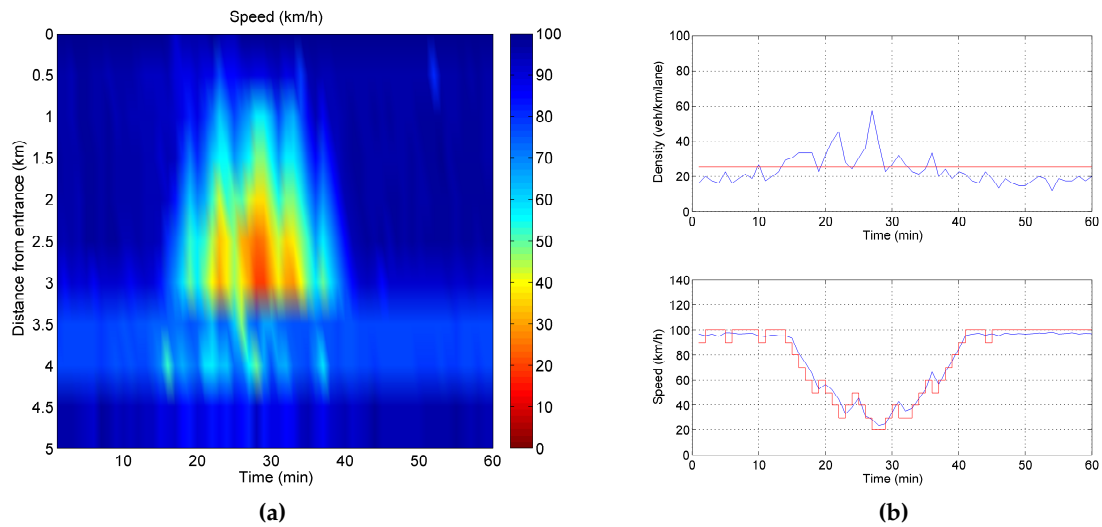
Figure 4.9: (a) Speed contour plot, (b) density measurements (blue line) at the bottleneck area (lane-drop area) with the corresponding critical density value (red line) and speed measurements at the MTFC application area with the corresponding speed limits (red line) for the VSL scenario

As Figure 4.10 displays the flow trajectory at the bottleneck area, capacity flow (3800 veh/h) is achieved for short periods of time without any capacity drop at the bottleneck area. Density is maintained around it's critical value (Figure 4.9(b)) even though it instantly reaches high values from t=22 min until t=28 min. On the other hand, penetration rate of 100% drives the VSL values ordered by the regulator (3.1) successfully. Congestion is elliminated earlier until t= 40 min with outflow being reduced accordingly to the decreased demand.

4.2.3 Lane Change Control Actions

In this scenario, the goal of the controller is to achieve a density distribution at the area downstream of the lane drop that will allow the full exploitation of capacity of
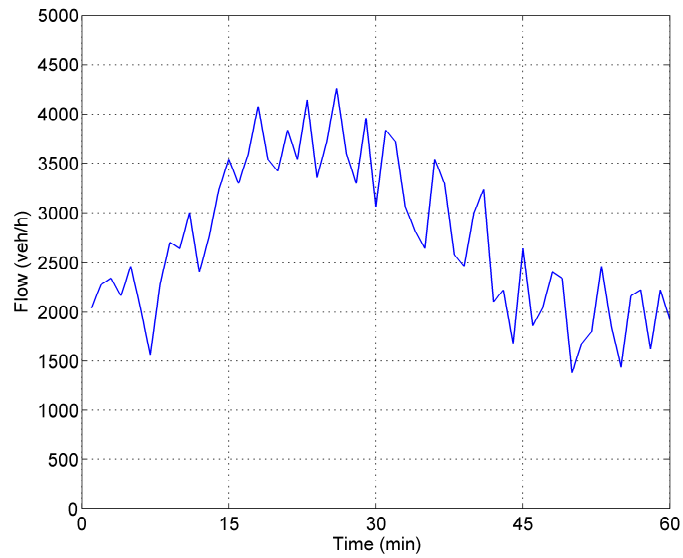
Figure 4.10: Outflow trajectory at the bottleneck area for the VSL scenario

each lane. This is done by delivering appropriate lateral flows by the linear feedback-feedforward control law (3.19) every 10 sec. Speed contour plots resulting from the LCC application at the present investigation are provided in Figure 4.11. The set-points used are 28 veh/km/lane for lane 2 and 33 veh/km/lane for lane 3 downstream of the lane-drop area.
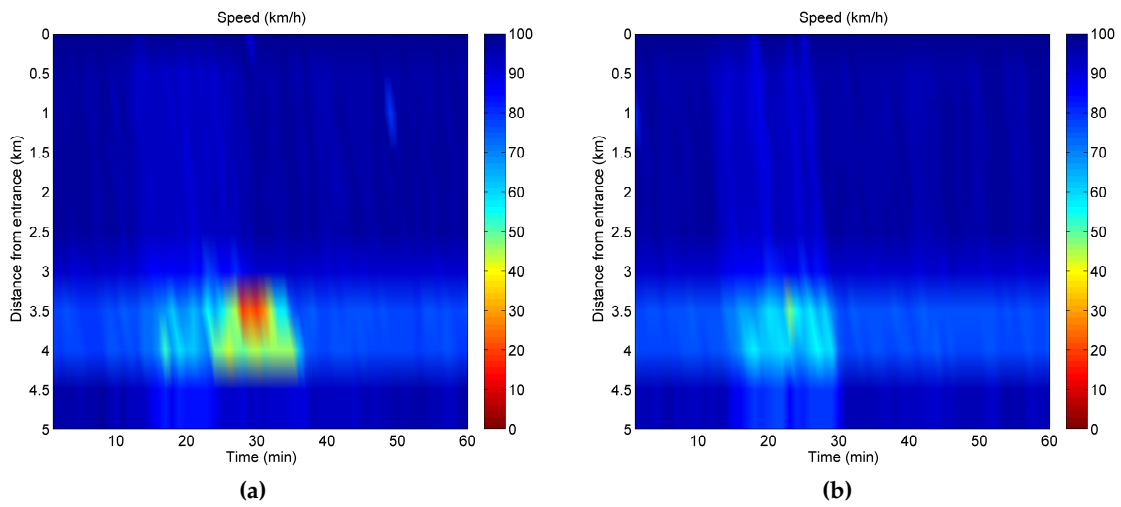
Figure 4.11: Speed contour plots for (a) 20% and (b) 80% of connected vehicles respectively for the LCC scenario

For a penetration rate of connected vehicles equal to 20% it can be seen from Figure 4.12(a) (when also compared with Figure 4.6(d)) that a higher outflow is achieved for lane 3 and that both lane 2 and lane 3 have a capacity around 2100 veh/h that is maintained for about 8 min.
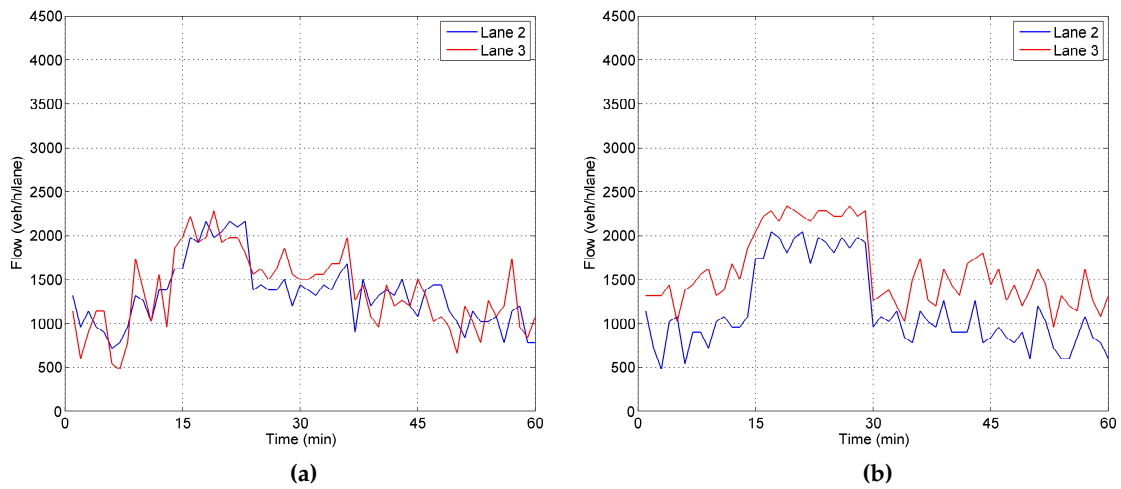
Figure 4.12: Per lane outflow trajectories at the bottleneck area (lane-drop area) for (a) 20% and (b) 80% of connected vehicles respectively for the LCC scenario

However, the lateral flows ordered by LCC can not be fully realized and the goal of the controller is not achieved for lane 3 (see Figure 4.13(a)). Congestion is then created due to further increasing demand, a capacity drop appears and a spillback of the queue covers almost 1 km upstream of the lane drop area. Nevertheless, a 14.6% improvement of the average TTS is obtained compared to the no-control case. As observed in Figure 4.8, the achieved improvement in TTS increases for higher penetration rates reaching 27%.

For a penetration rate of connected vehicles equal to 80%, it can be observed (Figure 4.12(b)) that even higher outflow values can be achieved for lane 3. This is because the lateral flows ordered by LCC can be realized and the goal of the controller is virtually achieved for a long period of time (see also Figure 4.13(b)). No congestion is created due to higher capacity values. The flow drop observed at $t = 30$ min is due to a decrease

of the demand.
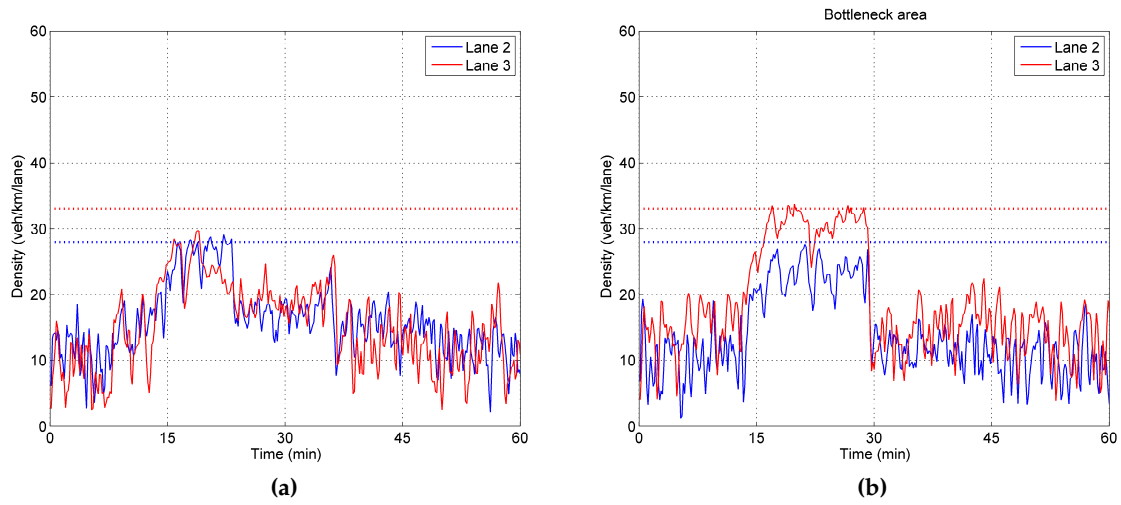
Figure 4.13: Per lane density trajectories (continuous lines) and corresponding set-points (dotted lines) downstream of the bottleneck area (lane-drop area) for (a) 20% and (b) 80% of connected vehicles for the LCC scenario

4.2.4 Integrated Scenario

In this case, MTFC is applied in addition to LCC to ensure that no congestion is created at the bottleneck and that the increased capacity due to LCC actions is maintained for longer periods of time. Speed contour plots are provided in Figure 4.14. Due to the increased capacity, higher set-points (35 veh/km/lane) are used in (3.1) for the density values. For a penetration rate of connected vehicles equal to 20%, there is an increased improvement compared to both previous non-integrated scenarios. As observed in Figure 4.15(a), VSL actions are still strong, without however reaching the minimum admissible value of 20 km/h. For a penetration rate of connected vehicles equal to 80%, VSL actions are more moderate (Figure 4.15(b)) and TTS values are virtually equal

to the ones obtained for the LCC scenario (see Figure 4.8).
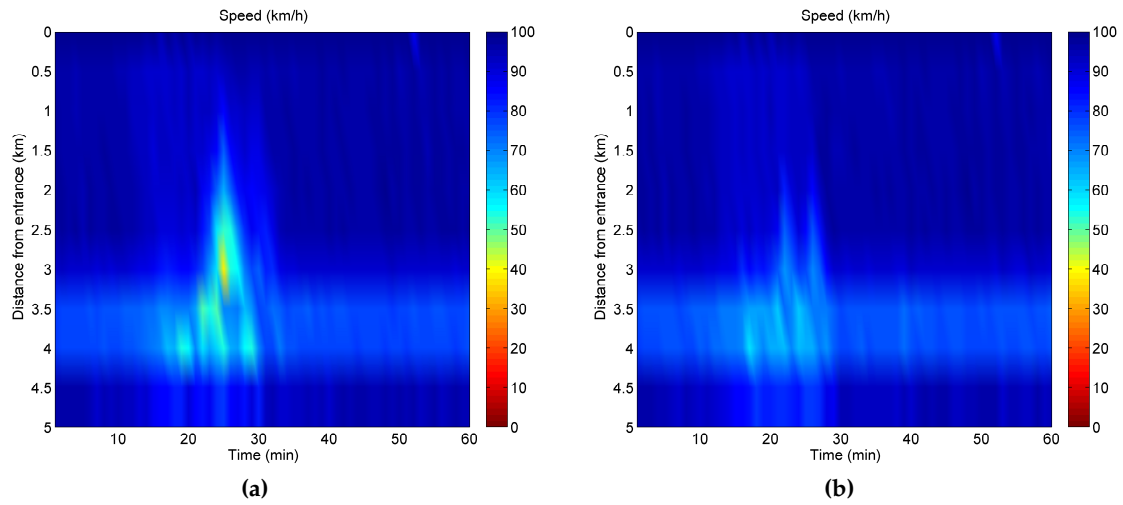
Figure 4.14: Speed contour plots for (a) 20% and (b) 80% of connected vehicles respectively for the integrated control scenario

Figure 4.16(a) demonstrates that for a penetration rate of 20% the increased capacity achieved for lane 3 is maintained for a longer period of time compared to the non-integrated (LCC only) scenario (see also Figure 4.12(a)). For a penetration rate of 80% the situation (Figure 4.16(b)) is similar to the non-integrated LCC scenario (Figure 4.12(b)).
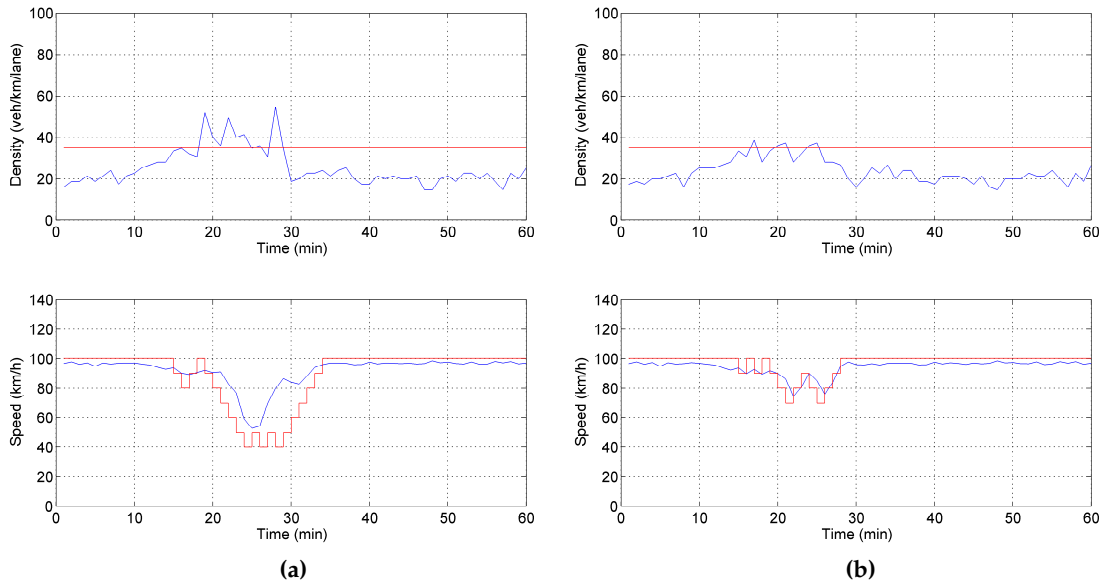
Figure 4.15: Density measurements (blue line) at the bottleneck area (lane-drop area) with the corresponding critical density value (red line) and speed measurements at the MTFC application area with the corresponding speed limits (red line) for (a) 20% and (b) 80% of connected vehicles for the integrated control scenario
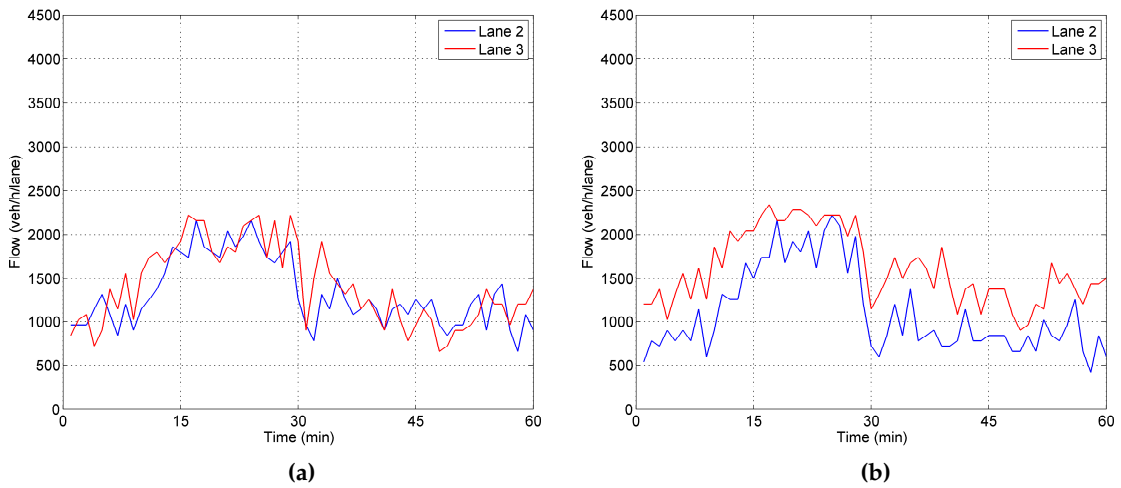
Figure 4.16: Per lane outflow trajectories at the bottleneck area for (a) 20% and (b) 80% of connected vehicles respectively for the integrated control scenario

A short appendix presenting the lane change formulation and the conducted results for other penetration rates, can be found in detail in A, B, C, D, E, F

4.2.5 Table Results

The control strategies scenarios are evaluated under the assumption of 20%, 40%, 60%, 80%, 100% penetration rates each with a set of ten replications. The average results are presented below the tables 4.3, 4.4, 4.5, 4.6, 4.7.

	Penetration rate 20%		
	TTT(veh·h)	TTT Improvement(%)	S.D.(veh·h)
No Control	223.3	-	13.9
VSL	208.9	6.45%	30.9
LCC	191.8	14.1%	23.8
Integrated	187.0	16.28%	20.4

Table 4.3: Average results for 20% penetration rate

	Penetration rate 40%		
	TTT(veh·h)	TTT Improvement(%)	S.D.(veh·h)
No Control	223.3	-	13.9
VSL	201.7	9.66%	12
LCC	170.6	23.59%	13.1
Integrated	169	24.31%	7.7

Table 4.4: Average results for 40% penetration rate

	Penetration rate 60%		
	TTT(veh·h)	TTT Improvement(%)	S.D.(veh·h)
No Control	223.3	-	13.9
VSL	200.6	10.19%	13.5
LCC	164.7	26.23%	5.7
Integrated	165.8	25.74%	5.6

Table 4.5: Average results for 60% penetration rate

	Penetration rate 80%		
	TTT(veh·h)	TTT Improvement(%)	S.D.(veh·h)
No Control	223.3	-	13.9
VSL	198.7	11.04%	14.6
LCC	161.6	27.65%	4.4
Integrated	163.1	26.98%	3.6

Table 4.6: Average results for 80% penetration rate

	Penetration rate 100%		
	TTT(veh·h)	TTT Improvement(%)	S.D.(veh·h)
No Control	223.3	-	13.9
VSL	199.5	10.68%	16.9
LCC	163.7	26.68%	4.6
Integrated	164.3	26.42%	4.6

Table 4.7: Average results for 100% penetration rate

Each table contains the Total Travel Time spent (TTT), Total Travel Time Improvement (TTT Improvement), Standard Deviation (S.D.) for each scenario and penetration rate, as examined for the set of 10 replications. The average result of TTS reduction, compared to the no-control case, reveal that the application of the VSL strategy is capable of mitigating congestion almost to 10%. However, when LCC actions are applied, even for low penetration rates a 14.1% improvement was obtained, reaching almost 27% at 100% penetration rate. Finally, when both strategies are applied (integrated scenario), no significant improvement was obtained for low penetration rates of 20%, 40%, 60%, while on the other hand, for 80% and 100% of connected vehicles the situation is similar to the non-integrated LCC scenario.

CHAPTER 5

Conclusion and future work

5.1 Conclusions

The objective of this master thesis was the evaluation of two previously proposed control strategies, namely the MTFC via VSL and the LCC, using a microscopic simulation model for a hypothetical lane-drop infrastructure. In order to test the effectiveness of each strategy, each scenario corresponds to each strategy as well. Also, the integrated use of the control strategies was tested, as the last scenario. Starting with the MTFC strategy, VSL, even for low penetration rates, have been proven successful in avoiding the capacity drop. On the other hand, the second strategy, LCC is able to achieve an appropriate lane assignment of vehicles upstream of the bottleneck and as a result increase its capacity. For low penetration rates of connected vehicles and for the demand profile used in this study, the conducted results validate that, the integrated use of the two strategies seems to be beneficial.

5.2 Future work

The produced results in this master thesis validate that the integrated use of the two proposed strategies applied on a 3 lane motorway with a lane-drop notion led to an elimination of congestion on the motorway with avoiding the capacity drop phenomena. Considering that a specific demand profile was tested for the productivity of the strategies, more work needs to be done to further improve the overall traffic conditions. For this reason, future work includes the evaluation of the integrated control structure for other bottleneck types, infrastructure layouts and demand profiles.

Bibliography

1. Roncoli, C., M. Papageorgiou, and I. Papamichail, Traffic flow optimisation in presence of vehicle automation and communication systems–Part I: A first-order multi-lane model for motorway traffic. *Transportation Research Part C: Emerging Technologies*, Vol. 57, 2015, pp. 241–259.

2. Roncoli, C., I. Papamichail, and M. Papageorgiou, Hierarchical model predictive control for multi-lane motorways in presence of vehicle automation and communication systems. *Transportation Research Part C: Emerging Technologies*, Vol. 62, 2016, pp. 117–132.

3. Knoop, V. L., A. Duret, C. Buisson, and B. Van Arem, Lane distribution of traffic near merging zones influence of variable speed limits. In *Proceedings of the 13th International IEEE Conference on Intelligent Transportation Systems*, 2010, pp. 485–490.

4. Roncoli, C., M. Papageorgiou, and I. Papamichail, Traffic flow optimisation in presence of vehicle automation and communication systems–Part II: Optimal control for multi-lane motorways. *Transportation Research Part C: Emerging Technologies*, Vol. 57, 2015, pp. 260–275.

5. Park, H., Byungkyu, Microscopic simulation model calibration and validation for freeway work zone network - a case study of vissim. *IEEE Transactions on Intelligent Transportation Systems*, Vol. 22, No. 3, 2006, pp. 1471–1476.

6. Systems, T. S., *Aimsun Dynamic Simulators User's Manual*. 8th ed., 2013.

7. Tapani, A., *Traffic simulation modelling of rural roads and driver assistance systems*. Ph.D. thesis, Linköping University Electronic Press, 2008.

8. Kesting, A. and M. Treiber, Calibrating car-following models by using trajectory data: Methodological study. *Transportation Research Record*, Vol. 2088, No. 1, 2008, pp. 148–156.

9. Gipps, P. G., A behavioural car-following model for computer simulation. *Transportation Research Part B: Methodological*, Vol. 15, No. 2, 1981, pp. 105–111.

10. Treiber, M., A. Hennecke, and D. Helbing, Congested traffic states in empirical observations and microscopic simulations. *Physical review E*, Vol. 62, No. 2, 2000, p. 1805.

11. Wang, J., R. Liu, and F. Montgomery, Car-following model for motorway traffic. *Transportation Research Record: Journal of the Transportation Research Board*, , No. 1934, 2005, pp. 33–42.

12. Mathew, T. V., Lane Changing Models. *Transportation systems engineering anonymous*, 2014, pp. 15.1–15.12.

13. Gipps, P. G., A model for the structure of lane-changing decisions. *Transportation Research Part B: Methodological*, Vol. 20, No. 5, 1986, pp. 403–414.

14. Chevallier, E. and L. Leclercq, Do microscopic merging models reproduce the ob-

served priority sharing ratio in congestion? *Transportation Research Part C: Emerging Technologies*, Vol. 17, No. 3, 2009, pp. 328–336.

15. Roncoli, C., I. Papamichail, and M. Papageorgiou, Model predictive control for multi-lane motorways in presence of VACS. In *Intelligent Transportation Systems (ITSC), 2014 IEEE 17th International Conference on*, IEEE, 2014, pp. 501–507.

16. Hidas, P., Evaluation of lane changing and merging in microsimulation models. In *Australasian Transport Research Forum (ATRF), 27th, 2004, Adelaide, South Australia, Australia*, 2004, Vol. 27.

17. Roncoli, C., N. Bekiaris-Liberis, and M. Papageorgiou, Lane-changing feedback control for efficient lane assignment at motorway bottlenecks. *Transportation Research Record: Journal of the Transportation Research Board*, , No. 2625, 2017, pp. 20–31.

18. Perraki, G., *Evaluation of a model predictive control strategy on a calibrated multilane microscopic model*, 2016.

19. Carlson, R. C., I. Papamichail, M. Papageorgiou, and A. Messmer, Optimal motorway traffic flow control involving variable speed limits and ramp metering. *Transportation Science*, Vol. 44, No. 2, 2010, pp. 238–253.

20. Papageorgiou, M., E. Kosmatopoulos, and I. Papamichail, Effects of variable speed limits on motorway traffic flow. *Transportation Research Record: Journal of the Transportation Research Board*, , No. 2047, 2008, pp. 37–48.

21. Carlson, R. C., I. Papamichail, M. Papageorgiou, and A. Messmer, Optimal mainstream traffic flow control of large-scale motorway networks. *Transportation Research Part C: Emerging Technologies*, Vol. 18, No. 2, 2010, pp. 193–212.

22. Carlson, R. C., I. Papamichail, and M. Papageorgiou, Comparison of local feedback controllers for the mainstream traffic flow on freeways using variable speed limits. *Journal of Intelligent Transportation Systems*, Vol. 17, No. 4, 2013, pp. 268–281.

23. Shinskey, F., Process control systems: application, design, and tuning. McGraw-Hill Co. *Inc., New York, NY*, 1996.

24. Diakaki, C., M. Papageorgiou, I. Papamichail, and I. Nikolos, Overview and analysis of vehicle automation and communication systems from a motorway traffic management perspective. *Transportation Research Part A: Policy and Practice*, Vol. 75, 2015, pp. 147–165.

25. Roncoli, C., N. Bekiaris-Liberis, and M. Papageorgiou, Optimal lane-changing control at motorway bottlenecks. In *Intelligent Transportation Systems (ITSC), 2016 IEEE 19th International Conference on*, IEEE, 2016, pp. 1785–1791.

26. Williams, R. L., D. A. Lawrence, et al., *Linear state-space control systems*. John Wiley & Sons, 2007.

27. Hespanha, J. P., *Linear systems theory*. Princeton University press, 2018.

28. Anderson, B., J. Moore, and B. Molinari, Linear optimal control. *IEEE Transactions on Systems, Man, and Cybernetics*, , No. 4, 1972, pp. 559–559.

APPENDIX A

Lane Change Formulation

$$A = \begin{bmatrix} 1 - \frac{T}{L_i}v_{i,j} & 0 & 0 & 0 & 0 & 0 & 0 & 0 & 0 \\ 0 & 1 - \frac{T}{L_i}v_{i,j} & 0 & 0 & 0 & 0 & 0 & 0 & 0 \\ 0 & 0 & 1 - \frac{T}{L_i}v_{i,j} & 0 & 0 & 0 & 0 & 0 & 0 \\ \frac{T}{L_i}v_{i-1,j} & 0 & 0 & 1 - \frac{T}{L_i}v_{i,j} & 0 & 0 & 0 & 0 & 0 \\ 0 & \frac{T}{L_i}v_{i-1,j} & 0 & 0 & 1 - \frac{T}{L_i}v_{i,j} & 0 & 0 & 0 & 0 \\ 0 & 0 & \frac{T}{L_i}v_{i-1,j} & 0 & 0 & 1 - \frac{T}{L_i}v_{i,j} & 0 & 0 & 0 \\ 0 & 0 & 0 & \frac{T}{L_i}v_{i-1,j} & 0 & 0 & 1 & 0 & 0 \\ 0 & 0 & 0 & 0 & \frac{T}{L_i}v_{i-1,j} & 0 & 0 & 1 - \frac{T}{L_i}v_{i,j} & 0 \\ 0 & 0 & 0 & 0 & 0 & \frac{T}{L_i}v_{i-1,j} & 0 & 0 & 1 - \frac{T}{L_i}v_{i,j} \end{bmatrix}$$

$$B = \begin{bmatrix} -\frac{T}{L_i} & 0 & 0 & 0 \\ \frac{T}{L_i} & -\frac{T}{L_i} & 0 & 0 \\ 0 & \frac{T}{L_i} & 0 & 0 \\ 0 & 0 & -\frac{T}{L_i} & 0 \\ 0 & 0 & \frac{T}{L_i} & -\frac{T}{L_i} \\ 0 & 0 & 0 & \frac{T}{L_i} \\ 0 & 0 & 0 & 0 \\ 0 & 0 & 0 & 0 \\ 0 & 0 & 0 & 0 \end{bmatrix}$$

$$C = \begin{bmatrix} 0 & 0 & 0 & 0 & 0 & 0 & 1 & 0 & 0 \\ 0 & 0 & 0 & 0 & 0 & 0 & 0 & 1 & 0 \\ 0 & 0 & 0 & 0 & 0 & 0 & 0 & 0 & 1 \end{bmatrix}$$

$$
Kx = \begin{bmatrix}
-22.8326 & 0.0741 & 0.0732 & 16.7527 & -0.2369 & 0.0297 & 31.7555 & -0.1114 & 0.0034 \\
-9.0636 & -8.8736 & 8.8932 & -5.9874 & -3.7053 & 3.6895 & -4.7483 & -0.5264 & 0.5175 \\
-104.6515 & 0.1374 & -0.0983 & -226.1840 & 0.6810 & -0.0027 & -264.1335 & 0.2644 & 0.0089 \\
-16.7325 & -17.0897 & 17.1158 & -26.9434 & -16.4388 & 16.4977 & -29.7597 & -4.7089 & 4.7292
\end{bmatrix}
$$

$$
Ky = \begin{bmatrix}
31.7555 & -0.1462 & 0.1462 \\
-4.7483 & -27.7628 & 27.7628 \\
-264.1335 & 0.4058 & -0.4058 \\
-29.7597 & -43.9453 & 43.9453
\end{bmatrix}
$$

$$
Kq = \begin{bmatrix}
71.0487 & -0.2094 & -0.0654 & 108.4112 & -0.3307 & -0.1852 & 80.9976 & 0.0570 & -0.2337 \\
23.8296 & 23.9851 & -23.9933 & 38.6610 & 38.5055 & -38.5458 & 48.4586 & 44.5686 & -44.5832 \\
5.3715 & 1.1078 & 0.5132 & 176.6193 & 0.8830 & 0.6741 & 546.7386 & -0.2314 & 0.6785 \\
9.6323 & 9.3400 & -9.1678 & 37.0128 & 37.3051 & -37.1755 & 81.1020 & 64.2050 & -64.1718
\end{bmatrix}
$$

$$
P = \begin{bmatrix}
1.6914 & 0.3804 & 0.1329 & 2.8381 & 0.2813 & 0.0801 & 3.1697 & 0.0718 & 0.0182 \\
0.3804 & 0.3825 & 0.1324 & 0.4674 & 0.2871 & 0.0802 & 0.4865 & 0.0739 & 0.0183 \\
0.1329 & 0.1324 & 0.3829 & 0.1291 & 0.0804 & 0.2875 & 0.1259 & 0.0184 & 0.0740 \\
2.8381 & 0.4674 & 0.1291 & 43.938 & 0.4442 & 0.0925 & 68.908 & 0.1270 & 0.0232 \\
0.2813 & 0.2871 & 0.0804 & 0.4442 & 0.6453 & 0.0569 & 0.4897 & 0.3154 & 0.0142 \\
0.0801 & 0.0802 & 0.2875 & 0.0925 & 0.0569 & 0.6461 & 0.0947 & 0.0142 & 0.3157 \\
3.1697 & 0.4865 & 0.1259 & 68.908 & 0.4897 & 0.0947 & 209.30 & 0.1431 & 0.0243 \\
0.0718 & 0.0739 & 0.0184 & 0.1270 & 0.3154 & 0.0142 & 0.1431 & 1.1744 & 0.0037 \\
0.0182 & 0.0183 & 0.0740 & 0.0232 & 0.0142 & 0.3157 & 0.0243 & 0.0037 & 1.1745
\end{bmatrix}
$$

APPENDIX B

No Control Scenario
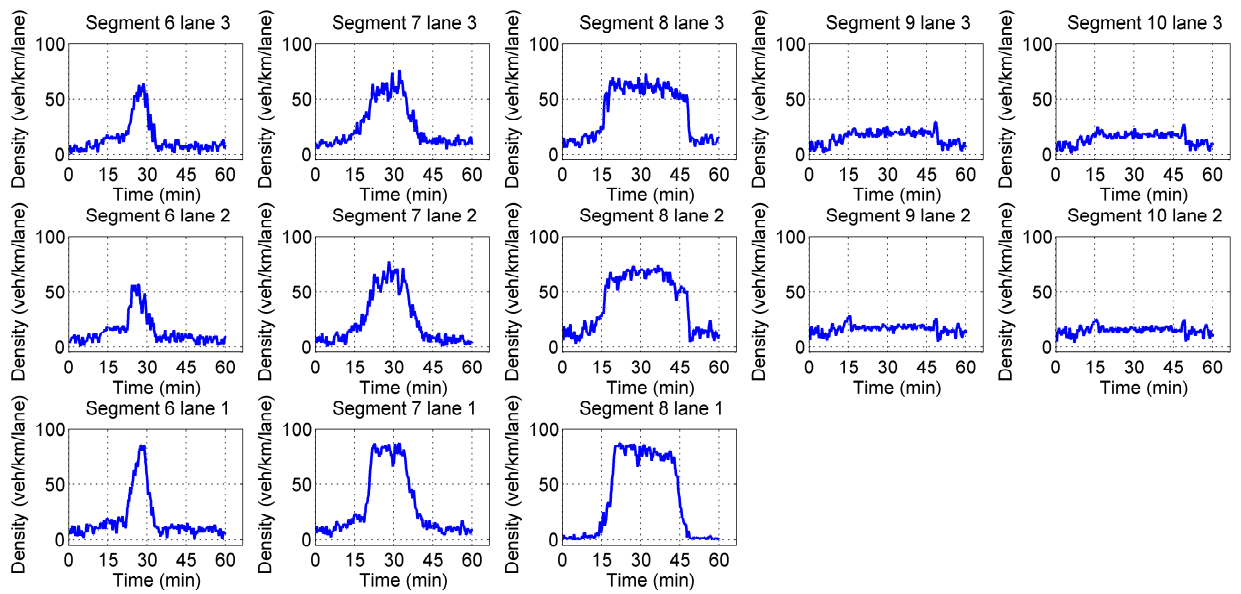
Figure B.1: Density trajectories for the no-control scenario
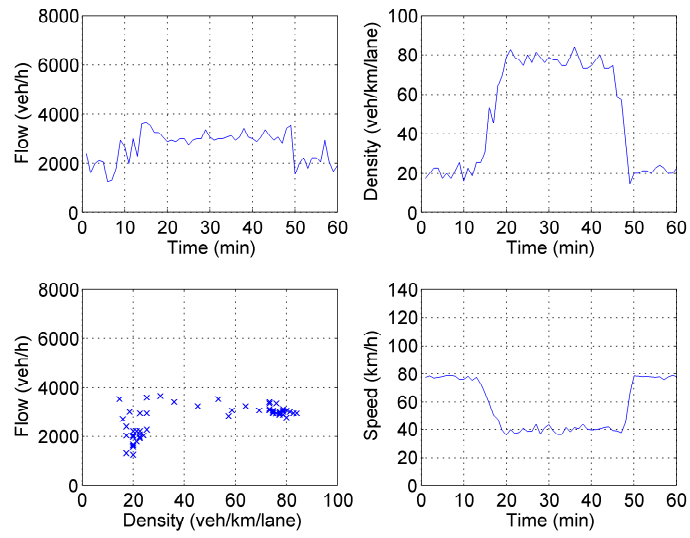
Figure B.2: State trajectories per lane at the bottleneck area for the no-control scenario

APPENDIX C

## Variable Speed Limits Scenario 100 % Penetration rate

---
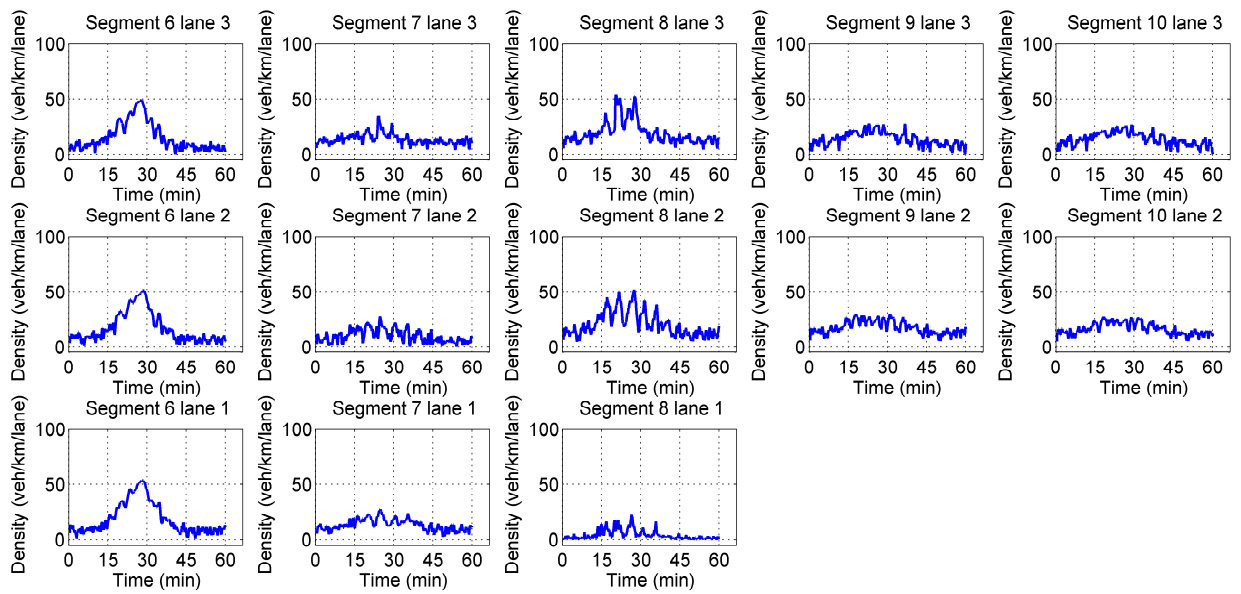
Figure C.1: Density trajectories for the VSL scenario
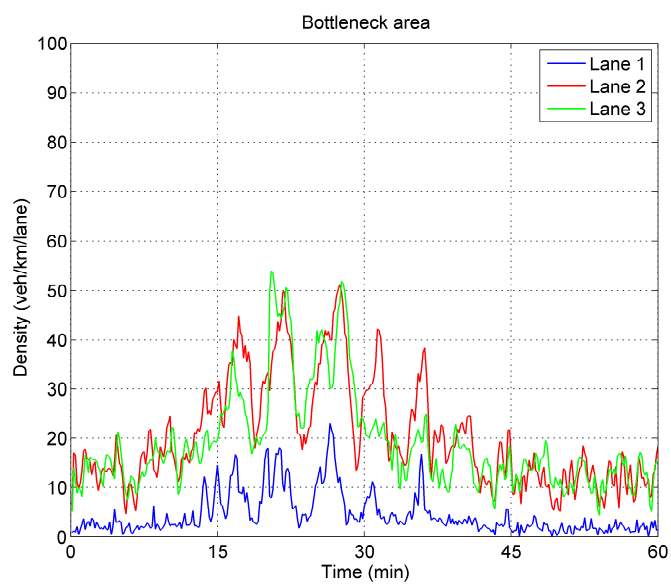
Figure C.2: Density trajectories per lane at the bottleneck area for the VSL scenario

APPENDIX D

Lane Change Control Actions 40% Penetration rate
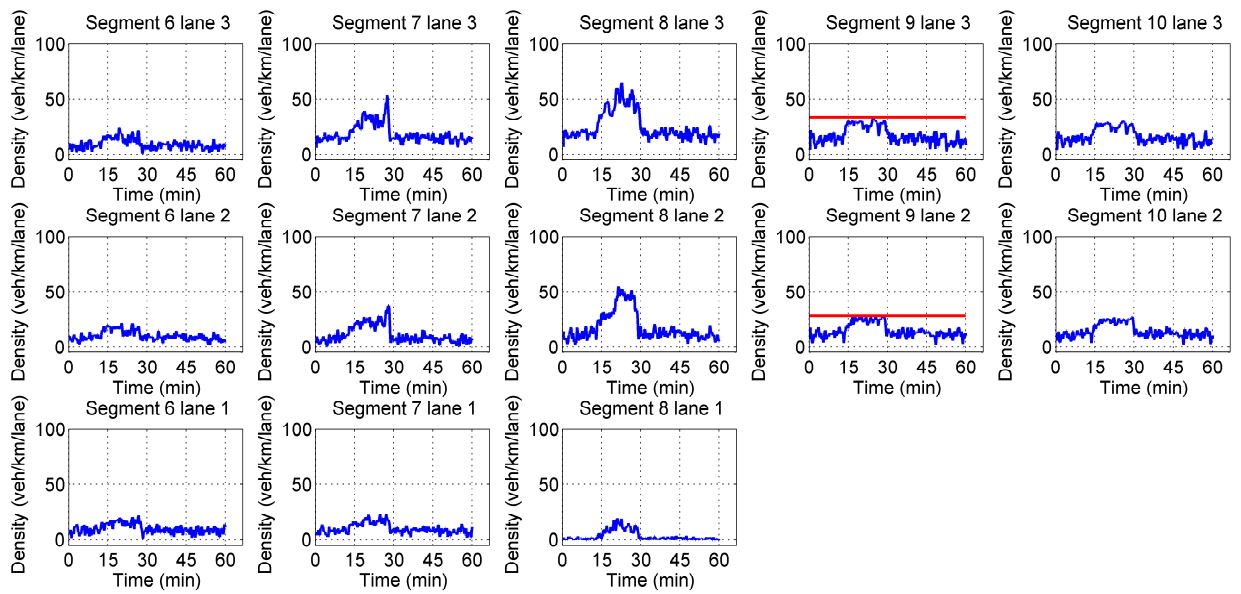
Figure D.1: Density trajectories for the LCC scenario and 40% penetration rate
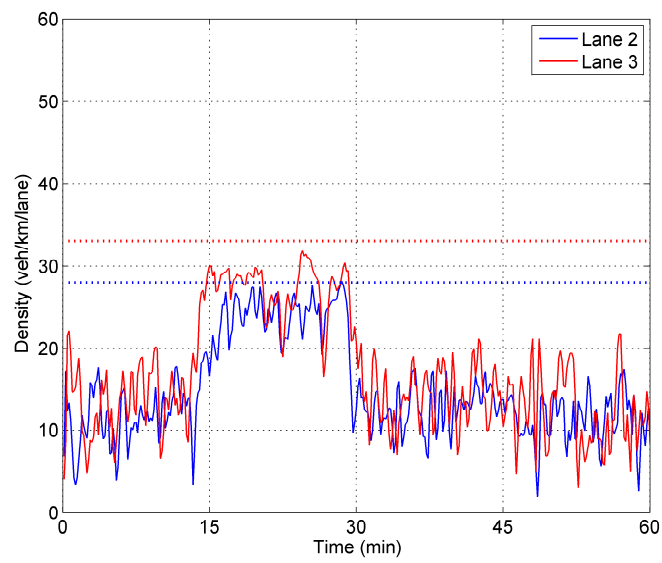
Figure D.2: Per lane density trajectories (continuous lines) and corresponding set-points (dotted lines) downstream of the bottleneck area for 40% of connected vehicles for the LCC scenario

APPENDIX E

## Lane Change Control Actions 60% Penetration rate

---
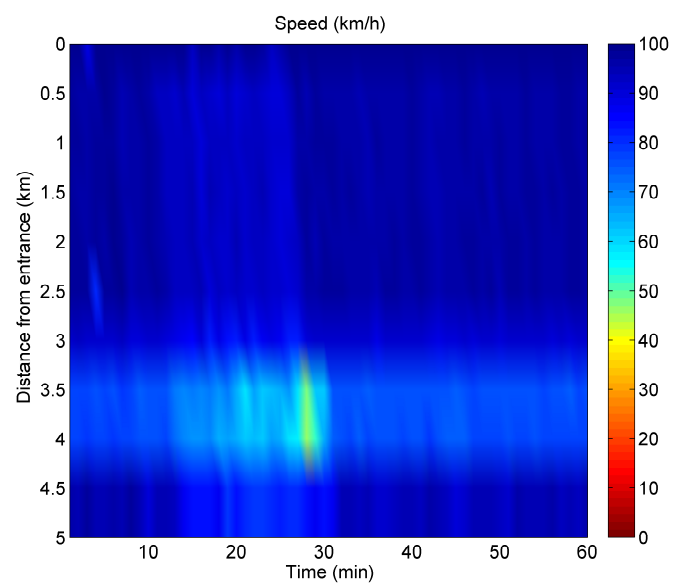
Figure E.1: Speed contour plot for the LCC scenario and 60% penetration rate
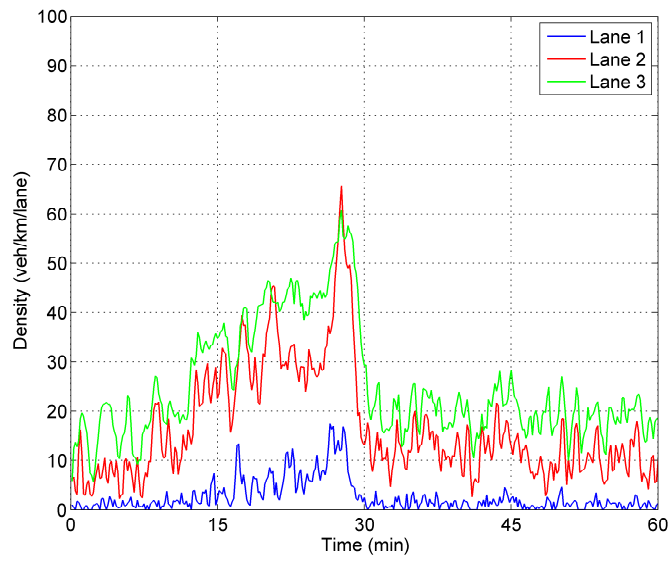
Figure E.2: Density trajectories per lane for the LCC scenario and 60% penetration rate
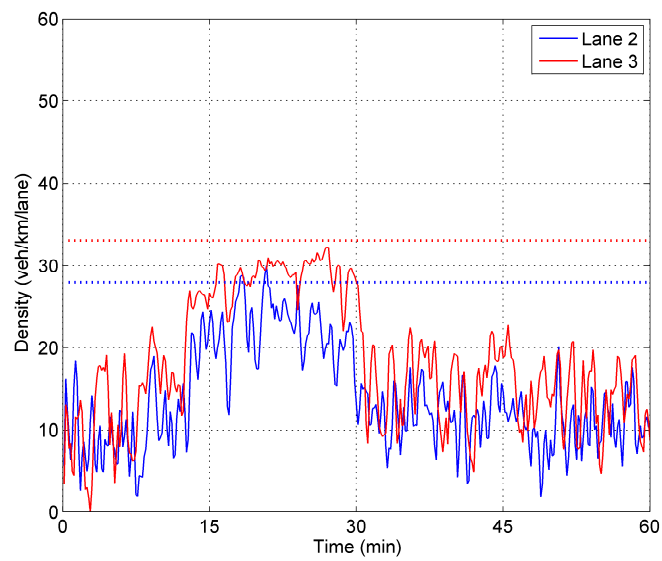

Figure E.3: Per lane density trajectories (continuous lines) and corresponding set-points (dotted lines) downstream of the bottleneck area for 60% of connected vehicles for the LCC scenario
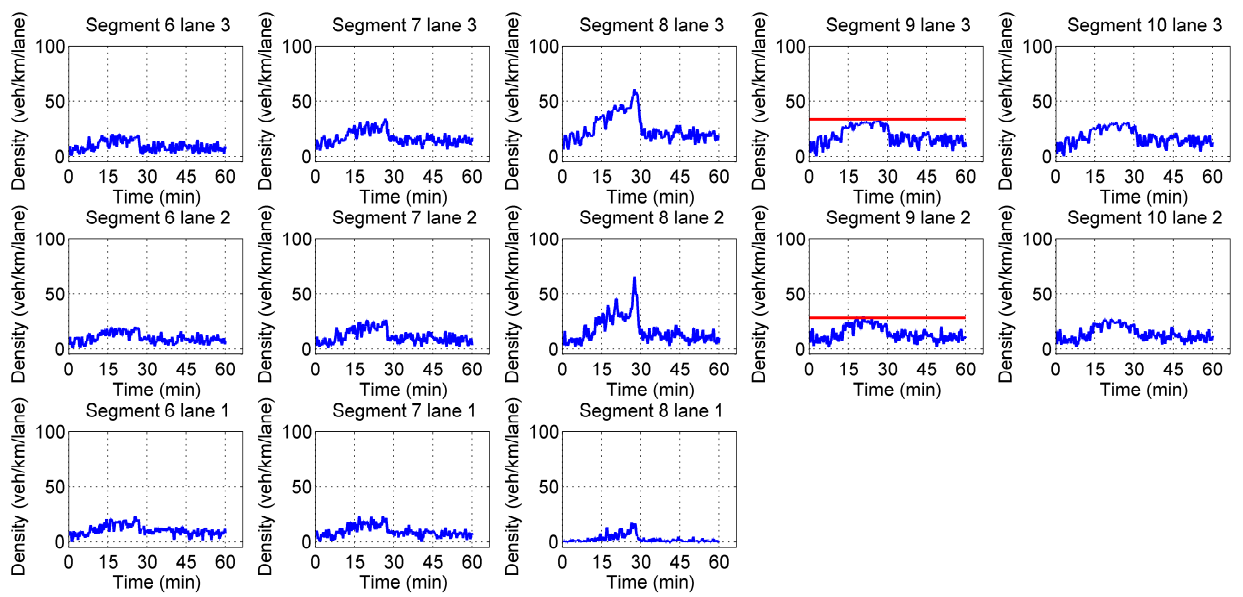
**Figure E.4:** Density trajectories for the LCC scenario and 60% penetration rate

APPENDIX F

Integrated Scenario 60% Penetration rate
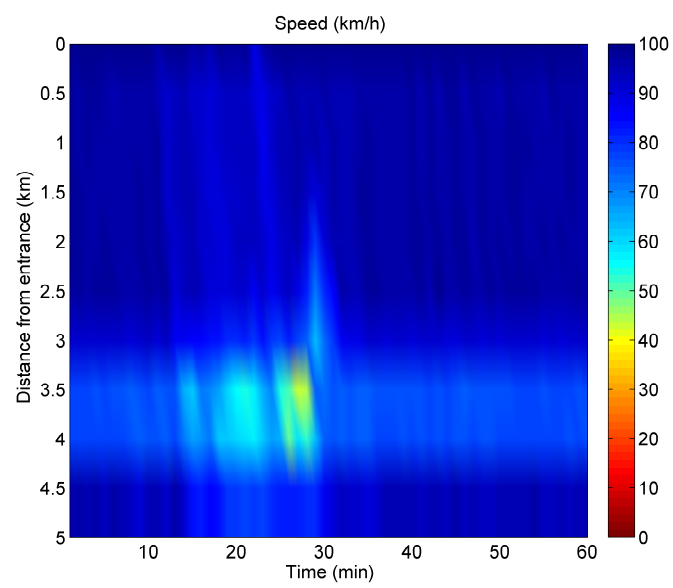
Figure F.1: Speed contour plot for the Integrated scenario and 60% penetration rate
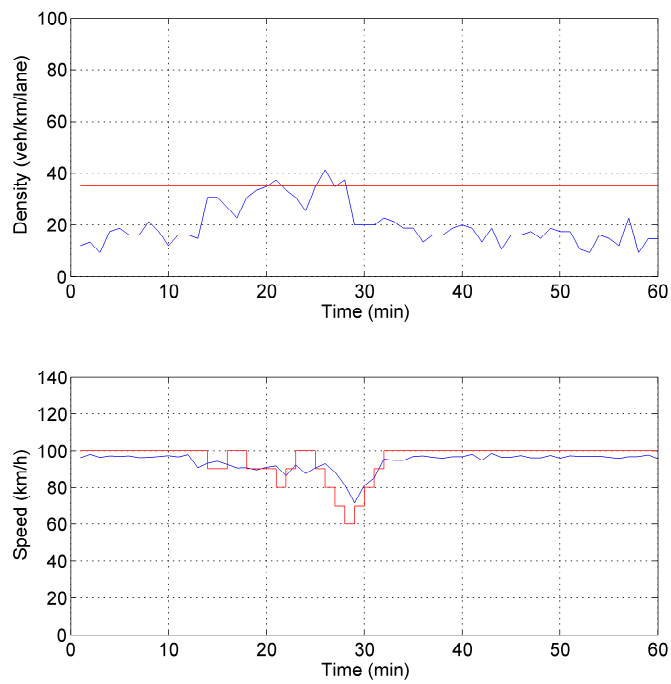
Figure F.2: Density measurements (blue line) at the bottleneck area (lane-drop area) with the corresponding critical density value (red line) and speed measurements at the MTFC application area with the corresponding speed limits (red line) for the Integrated 60% penetration rate scenario
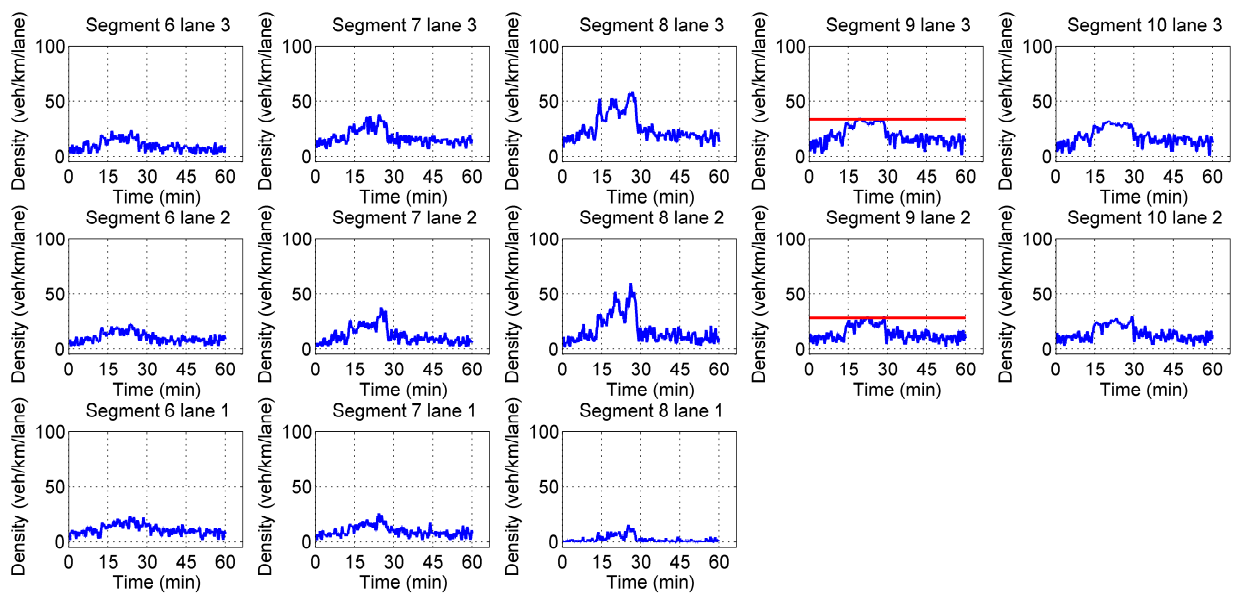
Figure F.3: Density trajectories for the Integrated scenario and 60% penetration rate